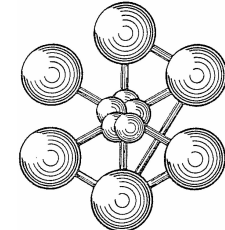


Club Castem 2011, 24 Novembre 2011, Vanves



GLOBAL-LOCAL X-FEM FOR 3D NON-PLANAR FRICTIONAL CRACK APPLICATION TO ROLLING FATIGUE

Gravouil A.⁽¹⁾, Trollé B.⁽¹⁾, Baietto M.-C.⁽¹⁾, Pierres E. ⁽¹⁾
Nguyen Thi Mac_Lan⁽²⁾, Mai Si Hai⁽²⁾
Prabel Benoit⁽³⁾, Fayard Jean-Luc⁽³⁾

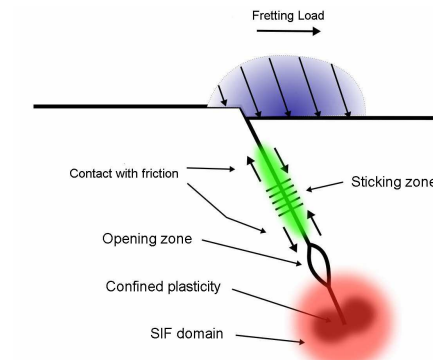
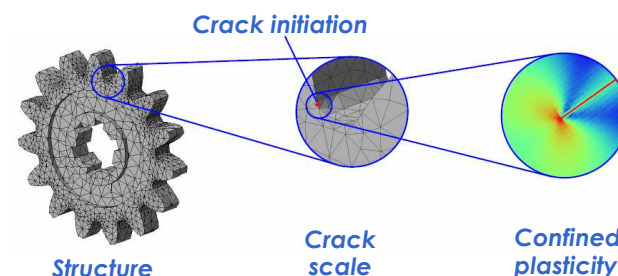
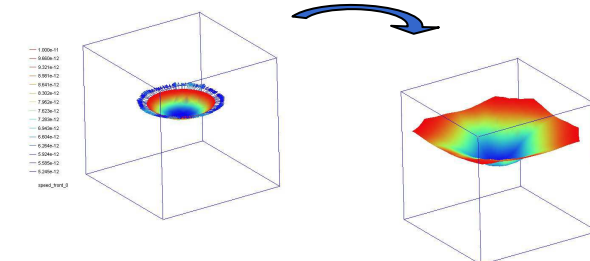
(1) LAMCOS

(2) SNCF / RATP

(3) CEA

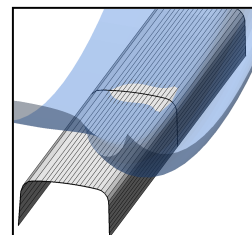
Introduction

- X-FEM coupled with a crack level set modelling greatly facilitates the simulation of 3D growing cracks
- Neither fine mesh (close to the front) nor remeshing of the domain (during the crack propagation) are required
- However, even with X-FEM, minimal requirements on the mesh design have to be taken into account. For instance:
 - Scale of the crack
 - Confined plasticity, closure effect
 - Localized non-linearities due to contact and friction along the crack faces

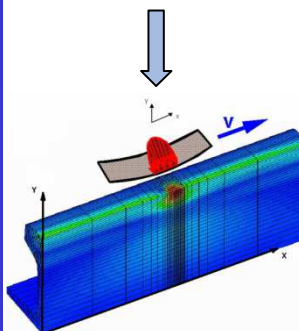


- When contact and friction occur along the crack faces, a discretization of the interface is required
- This involves a mesh dependency between the interface and the structure

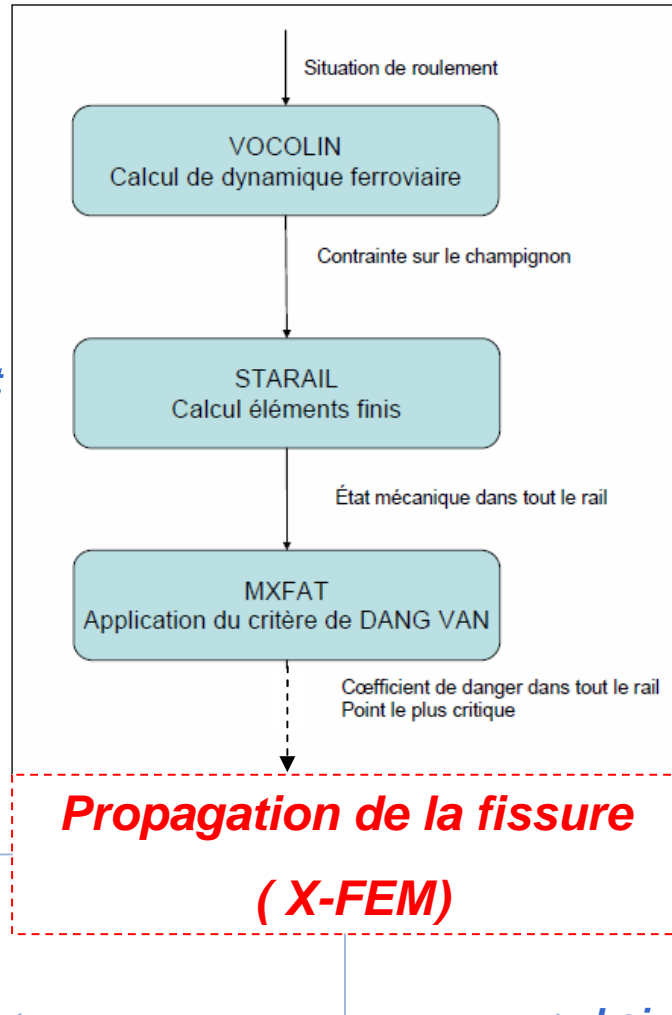
Introduction



Contact et frottement
entre les lèvres de la
fissure



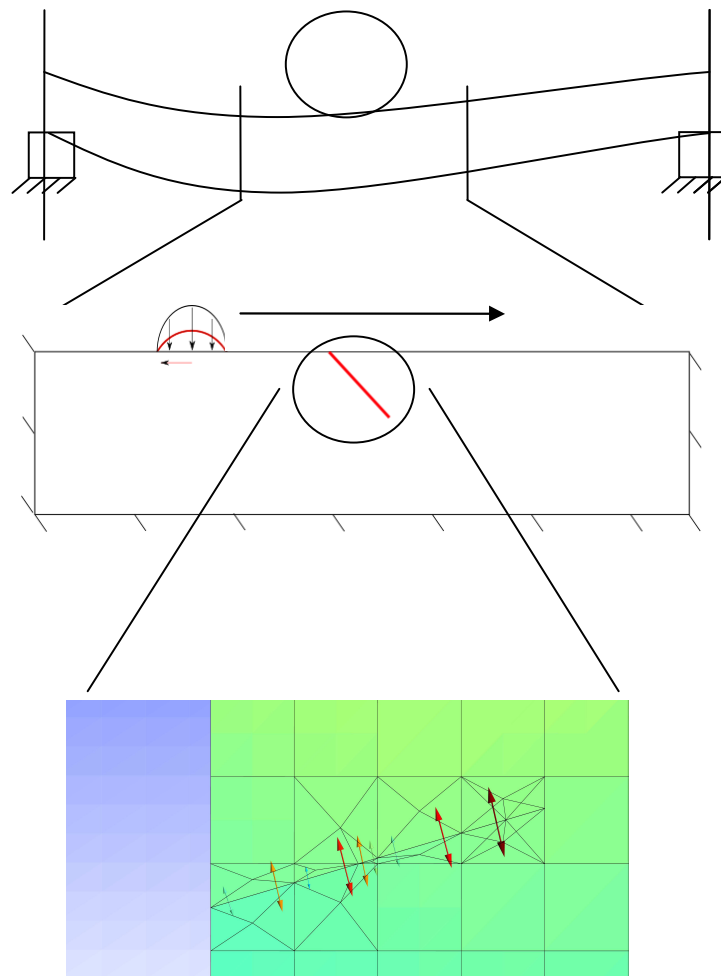
Chargement
multi-axial
Non proportionnel



Loi de propagation
dédiée

Contraintes
résiduelles

Stratégie multi-échelle pour la simulation de la propagation des fissures



Échelle de la structure

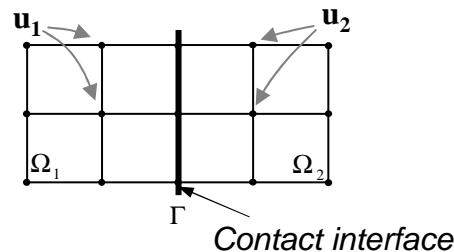
*Échelle de la
discontinuité
géométrique*

*Échelle du contact et du
frottement entre les
lèvres de la fissure*

Modelling of the interfacial Fictrional contact with X-FEM

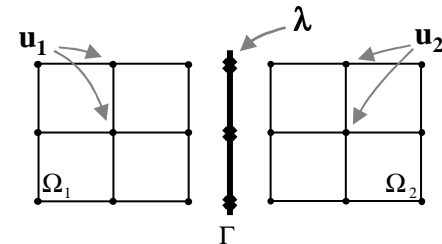
- Three mainly formulations of the contact problem with X-FEM:

- Primal formulation:



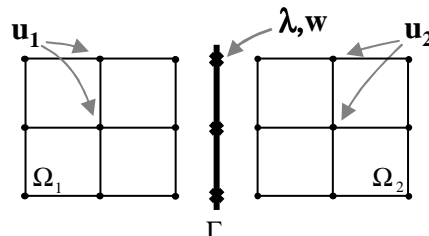
[F. Liu, R.I. Borja, IJNME 2008]

- Dual formulation:



[F. Liu, R.I. Borja, CMAME 2010]
 [E. Giner, M. Tur, J. E. Tarancón, F.J. Fuenmayor, IJNME 2009]
 [N. Moës, B. Béchet, M. Tourbier, IJNME 2006]
 [E. Béchet, N. Moës, B. Wohlmuth, IJNME 2009]
 [I. Nistor, M.L.E. Guiton, P. Massin, N. Moës et al., IJNME 2009]
 [S. Géniaut, P. Massin, N. Moës, EJCM 2007]

- Mixed formulation:

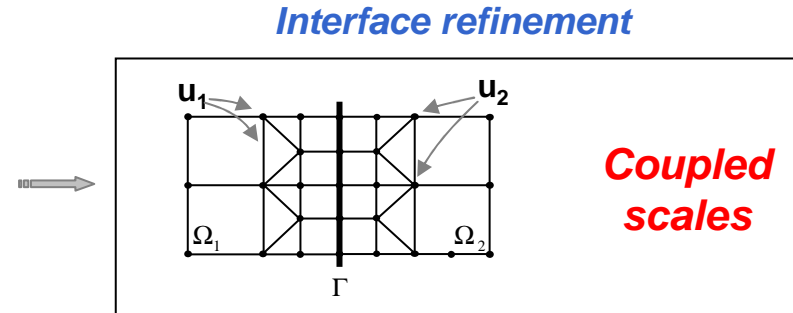
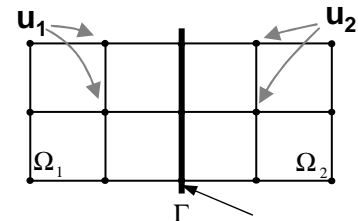


[J. Dolbow, N. Moës, T. Belytschko, CMAME 2001]
 [T. Elguedj, A. Gravouil, A. Combescure, IJNME 2007]
 [R. Ribeaucourt, M.C. Baietto Dubourg, A. Gravouil, CMAME 2007]

Modelling of the interfacial Frictional contact with X-FEM

- Three mainly formulations of the contact problem with X-FEM:

- Primal formulation:

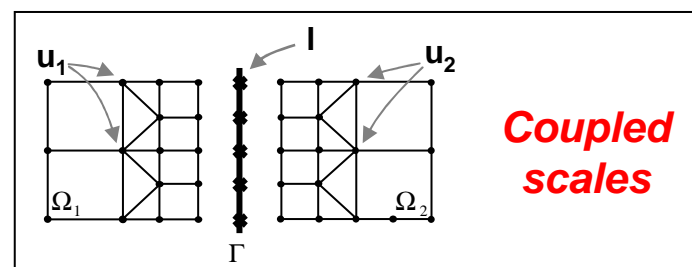
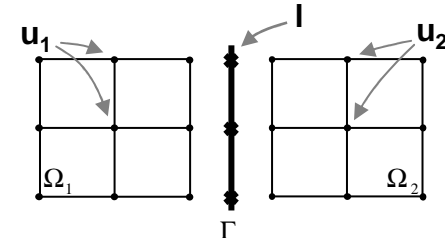


Coupled scales

Stability

Unconditionally stable

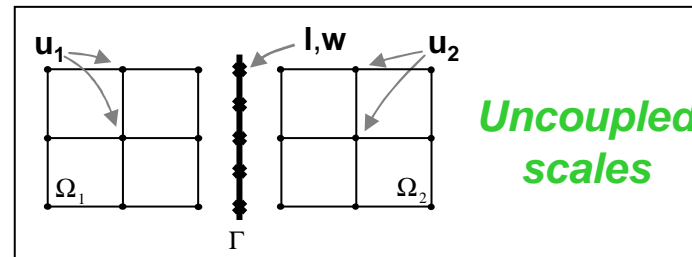
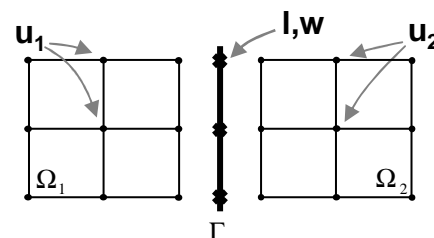
- Dual formulation:



Coupled scales

Conditionally stable

- Mixed formulation:



Uncoupled scales

Conditionally stable

OUTLINE

- 1 *X-FEM with level sets for 3D crack growth simulation*
- 2 *A 3 field weak formulation + 2 scales strategy*
- 3 *Examples (ELFE_3D: LaMCoS in-house Software + GMSH)*
- 4 *Applications – Cast3m implementation*
- 5 *Conclusions & perspectives*

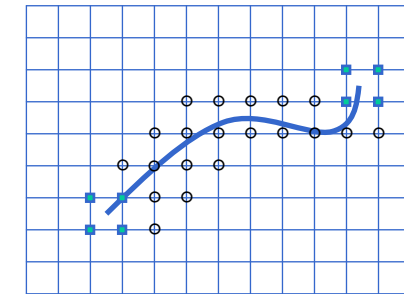
1

Xtended Finite Element Method + level sets

- Local partition of unity (two scale strategy):

- Discontinuous and asymptotic enrichment of the displacement field

$$(\) \sum (\) \sum (\) (\) \sum \sum (\) (\) \\ \{ \ } \{ \sqrt{-}(-) \sqrt{-}(-) \sqrt{-}(-) (\) \sqrt{-}(-) (\) \}$$

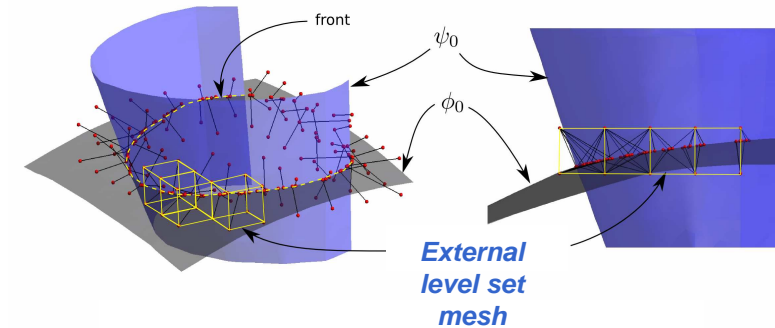


- Crack shape modeling by two level sets:

$$(\) \quad (\) \quad \text{crack} \\ (\) \quad (\) \quad \text{Crack front}$$

- Level set update — | |

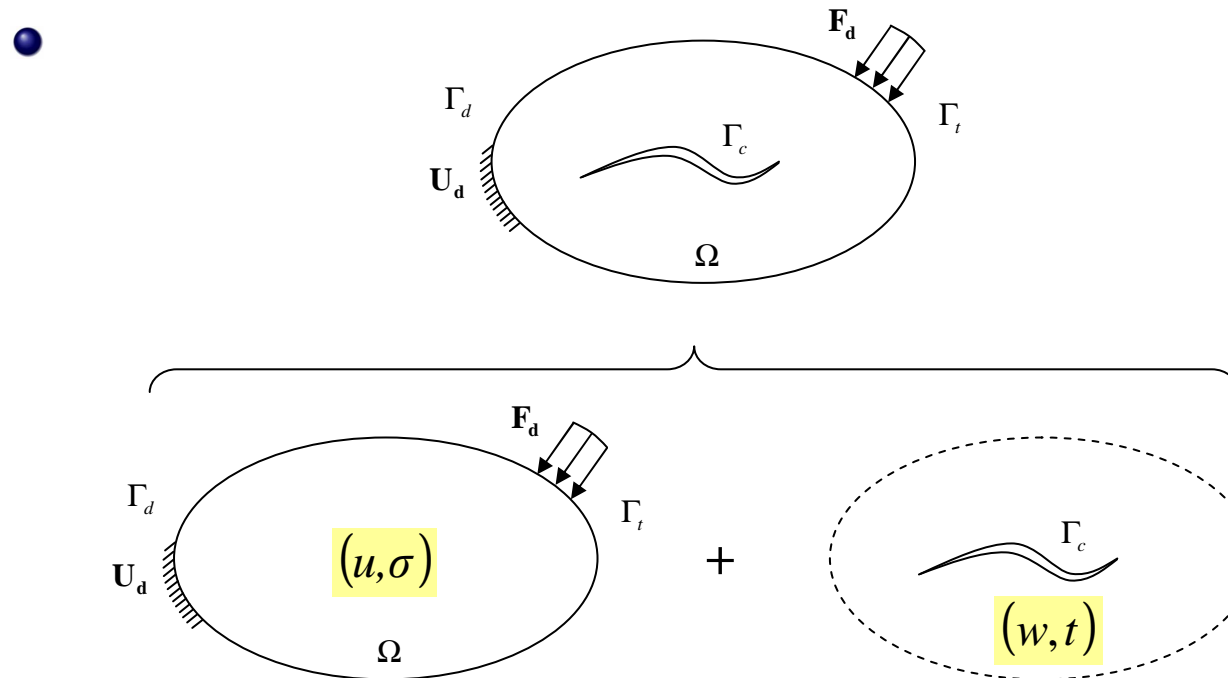
- Local orthogonality



[Moës 1999, Stolarska 2001, Duflot 2005, Béchet 2005, Sukumar 2007] [Rannou 2009]

[Gravouil A., Moës N., Belytschko T., IJNME, 2002] [Sethian 1997]

2 Two scales strategy (Structure / crack)



● Global problem (u, σ)

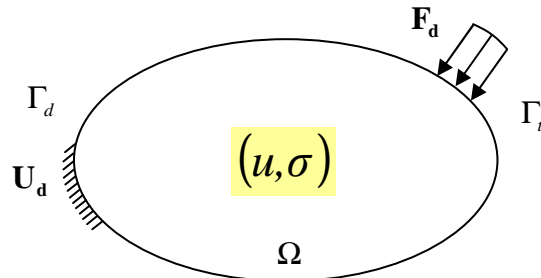
Scale of the structure
Equilibrium and constitutive law
in the bulk (possibly nonlinear)

● Local problem (w, t)

Scale of the crack
Constitutive law at the interface
(unilateral contact, contact with friction)

2 Two scale strategy: three field weak formulation

- Global problem

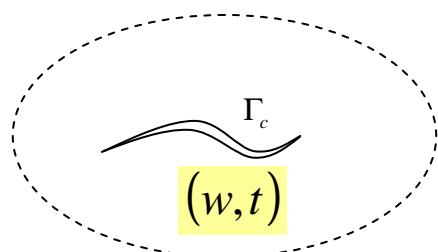


$$P_{int}^* = - \int_{\Omega} \boldsymbol{\sigma}(t) : \boldsymbol{\epsilon}(\mathbf{u}^*) d\Omega$$

$$P_{ext}^* = \int_{\Gamma_t} \mathbf{f}_t(t) \cdot \mathbf{u}^* dS$$

+ constitutive law in the bulk on (u, σ) (possibly nonlinear)

- Local problem



$$P_{crack}^* = \int_{\Gamma_C} \mathbf{t}(t) \cdot \mathbf{w}^* dS$$

+ interface constitutive law on (w, t) (unilateral, frictional contact)

- Coupling between local and global problems

Strong formulation:

Weak coupling:

$$\begin{aligned} \boldsymbol{\sigma}(t) \cdot \mathbf{n} &= \mathbf{t}^+(t) \quad \text{on } \Gamma_C^+ \quad \text{and} \quad \boldsymbol{\sigma}(t) \cdot -\mathbf{n} = \mathbf{t}^-(t) \quad \text{on } \Gamma_C^- \\ \mathbf{u}(t) &= \mathbf{w}^+(t) \quad \text{on } \Gamma_C^+ \quad \text{and} \quad \mathbf{u}(t) = \mathbf{w}^-(t) \quad \text{on } \Gamma_C^- \end{aligned}$$

$$P_{coupling}^* = \int_{\Gamma_C} \boldsymbol{\lambda}^* \cdot (\mathbf{u}(t) - \mathbf{w}(t)) dS + \int_{\Gamma_C} \boldsymbol{\lambda}(t) \cdot (\mathbf{u}^* - \mathbf{w}^*) dS$$

2 Two scale strategy: three field weak formulation

- Principle of virtual works:

$$P_{int}^* + P_{ext}^* + P_{crack}^* + P_{coupling}^* = 0$$

$$\forall \mathbf{u}^* \in U_0^*, \forall \mathbf{w}^* \in W^*, \forall \boldsymbol{\lambda}^* \in \Lambda^*, \forall t \in [0; T]$$

- Three field weak formulation of the fracture problem with frictional contact between the crack faces:

$$\left\{ \begin{array}{l} 0 = - \int_{\Omega} \boldsymbol{\sigma}(t) : \boldsymbol{\epsilon}(\mathbf{u}^*) d\Omega + \int_{\Gamma_t} \mathbf{f}_t(t) \cdot \mathbf{u}^* dS + \int_{\Gamma_C} \boldsymbol{\lambda}(t) \cdot \mathbf{u}^* dS \\ \quad + \int_{\Gamma_C} (\mathbf{t}(t) - \boldsymbol{\lambda}(t)) \cdot \mathbf{w}^* dS \\ \quad + \boxed{\int_{\Gamma_C} (\mathbf{u}(t) - \mathbf{w}(t)) \cdot \boldsymbol{\lambda}^* dS} \end{array} \right. \quad \boxed{\text{Weak coupling between } u \text{ and } w}$$

$\forall \mathbf{u}^* \in U_0^*, \forall \mathbf{w}^* \in W^*, \forall \boldsymbol{\lambda}^* \in \Lambda^*, \forall t \in [0; T]$

- + Constitutive law in volume (u, σ) (possibly non linear)
- + Frictional contact law at the interface (w, t)

→ Allows an intrinsic description - with its own primal and dual variables (w, t)
 of the crack interface: - with its own (possibly refined) discretization

2

Discretized three field weak formulation

- *X-FEM discretization of the displacement field in the bulk*

$$\mathbf{u}(\mathbf{x}, t) \simeq \sum_{i \in N_{nodes}} \mathbf{u}_i(t) \Phi_i(\mathbf{x}) + H(\mathbf{x}) \cdot \sum_{j \in N_{crack}} \mathbf{a}_j(t) \Phi_j(\mathbf{x}) + \sum_{l=1} B_l \cdot \sum_{k \in N_{front}} \mathbf{b}_{lk}(t) \Phi_k(\mathbf{x})$$

- *Discretization of the displacement and load field on the interface*

$$\mathbf{w}(\mathbf{x}, t) \simeq \sum_{i=1}^3 \mathbf{w}_i(t) \Psi_i(\mathbf{x})$$

$$\mathbf{t}(\mathbf{x}, t) \simeq \sum_{i=1}^3 \mathbf{t}_i(t) \Psi'_i(\mathbf{x})$$

$$\boldsymbol{\lambda}(\mathbf{x}, t) \simeq \sum_{i=1}^3 \boldsymbol{\lambda}_i(t) \Psi'_i(\mathbf{x})$$

- *Discretized 3 field weak formulation*

*(mortar method)
(unambiguously definition
of the coefficients)*

$$0 = +\mathbf{U}^{*T}(-\mathbf{F}_{int}(\mathbf{U}(t)) + \mathbf{F}_{ext}(t) + \mathbf{L}^T \boldsymbol{\Lambda}(t))$$

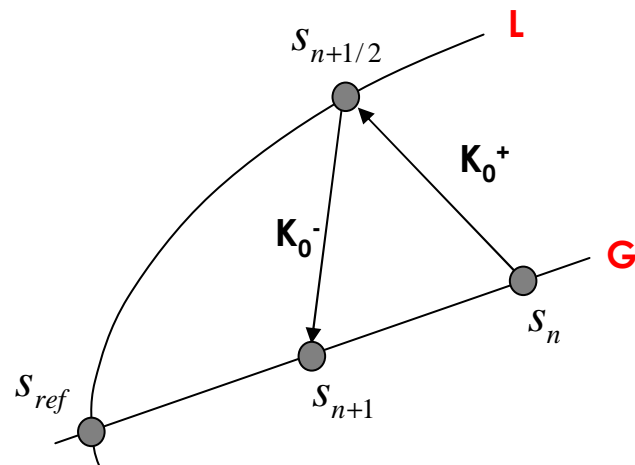
$$+ \mathbf{W}^{*T}(\mathbf{T}(t) - \boldsymbol{\Lambda}(t))$$

$$+ \boldsymbol{\Lambda}^{*T}(\mathbf{L}\mathbf{U}(t) - \mathbf{W}(t))$$

2

Non linear iterative solver (LATIN method)

- *Iterative solver for the solution of the frictional contact problem $s = (u, \omega, t)$ (incremental LATIN Method [Ladevèze 1985])*
 - *divide the equations into two subsets :*
 - *global linear equations (G) (3 field weak formulation)*
 - *local possibly non linear equations (L) (frictional contact equations)*
 - *find an approximate solution according to an iterative process in 2 stages*
- *Iterative strategy:*
- *Corresponding search directions:*



$$t_{i+\frac{1}{2}} - t_i = \mathbf{K}_0(\omega_{i+\frac{1}{2}} - \omega_i)$$

$$t_{i+1} - t_{i+\frac{1}{2}} = -\mathbf{K}_0(\omega_{i+1} - \omega_{i+\frac{1}{2}})$$

$$\mathbf{K}_0 = k_0 Id$$

2

Non linear iterative solver (LATIN method) Global stage (3 field weak formulation)

- **Combination of the 3 field weak formulation and the search direction:**

$$\begin{aligned}
 0 = & - \int_{\Omega} \boldsymbol{\sigma}_{i+1} : \boldsymbol{\epsilon}(\mathbf{u}^*) d\Omega + \int_{\Gamma^t} \mathbf{f}_t \cdot \mathbf{u}^* dS + \int_{\Gamma_C} \boldsymbol{\lambda}_{i+1} \cdot \mathbf{u}^* dS \\
 & + \int_{\Gamma_C} (\mathbf{t}_{i+\frac{1}{2}} + k_0 \mathbf{w}_{i+\frac{1}{2}}) \cdot \mathbf{w}^* dS - \int_{\Gamma_C} (\boldsymbol{\lambda}_{i+1} + k_0 \mathbf{w}_{i+1}) \cdot \mathbf{w}^* dS \\
 & + \int_{\Gamma_C} (\mathbf{u}_{i+1} - \mathbf{w}_{i+1}) \cdot \boldsymbol{\lambda}^* dS \quad \forall \mathbf{u}^* \in U_0^*, \quad \forall \mathbf{w}^* \in W^* \text{ and } \forall \boldsymbol{\lambda}^* \in \Lambda^*
 \end{aligned}$$

- **Corresponding linear system:**

$$\left[\begin{array}{ccc} \mathbf{K} & 0 & -\mathbf{K}_{u\lambda} \\ 0 & \mathbf{K}_{ww} & \mathbf{K}_{w\lambda} \\ -\mathbf{K}_{u\lambda}^T & \mathbf{K}_{w\lambda}^T & 0 \end{array} \right] \left(\begin{array}{c} \mathbf{U}_{i+1} \\ \mathbf{W}_{i+1} \\ \boldsymbol{\Lambda}_{i+1} \end{array} \right) = \left(\begin{array}{c} \mathbf{F}_t \\ \mathbf{K}_{w\lambda} \cdot \mathbf{T}_{i+\frac{1}{2}} + \mathbf{K}_{ww} \cdot \mathbf{W}_{i+\frac{1}{2}} \\ 0 \end{array} \right)$$

Mortar operators: coupling in a weak sense of interface-structure non-matching discretization

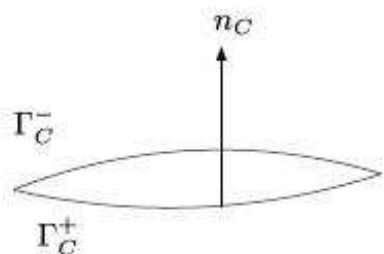
- **Very close to the augmented Lagrangian formulation [Elguedj 2007]:**

$$\left[\begin{array}{ccc} \mathbf{K} & 0 & -\mathbf{K}_{u\lambda} \\ 0 & \mathbf{K}_{ww} & \mathbf{K}_{w\lambda} \\ -\mathbf{K}_{u\lambda}^T & \mathbf{K}_{w\lambda}^T & 0 \end{array} \right] \left(\begin{array}{c} \Delta \mathbf{U}_{i+1} \\ \Delta \mathbf{W}_{i+1} \\ \Delta \boldsymbol{\Lambda}_{i+1} \end{array} \right) = \left(\begin{array}{c} \mathbf{F}_t + \mathbf{K}_{u\lambda} \cdot \boldsymbol{\Lambda}_i \\ \mathbf{K}_{w\lambda} \cdot (\mathbf{T}_i - \boldsymbol{\Lambda}_i) \\ \mathbf{K}_{u\lambda}^T \cdot \mathbf{U}_i - \mathbf{K}_{w\lambda}^T \cdot \mathbf{W}_i \end{array} \right)$$

2

Non linear iterative solver (LATIN method)

Local stage (frictional contact equations)

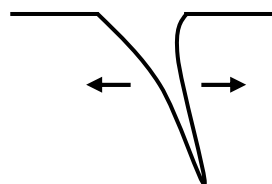


- *Notations for the local interface fields:*

$$[w] = \omega^- - \omega^+$$

$$\Delta w = \omega^n - \omega^{n-1}$$

$$\Delta [w_T] = \Delta \omega_T^{-n} - \Delta \omega_T^{+n} = (\omega_T^{-n} - \omega_T^{+n}) - (\omega_T^{-(n-1)} - \omega_T^{+(n-1)})$$



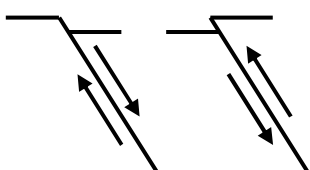
- *Unilateral contact at crack interface (w, t)*

$$[w_N] := \omega_N^- - \omega_N^+ \geq 0$$

$$F_N := t_N^+ = -t_N^- \leq 0$$

$$F_T := t_T^+ = -t_T^-$$

$$[w_N].F_N = 0$$



- *Frictional conditions at crack interface (w, t)*

$$\| F_T \| < \mu_C | F_N | \Rightarrow \Delta [w_T] = 0$$

$$\| F_T \| = \mu_C | F_N | \Rightarrow \exists \lambda \geq 0, \Delta [w_T] = \lambda F_T$$

2

Specific convergence indicator

● **Convergence indicator:**

- *distance between the global and local approximations*
- *allows to stop the iterative process when the error is lower than a prescribed tolerance*
- *ensures the convergence both on the normal and tangential problems*

$$\eta_N = \frac{\| s_{N,i+1} - s_{N,i+\frac{1}{2}} \|_{\infty}^2}{\| s_{N,i+1} \|_{\infty}^2 + \| s_{N,i+\frac{1}{2}} \|_{\infty}^2} , \quad \eta_T = \frac{\| s_{T,i+1} - s_{T,i+\frac{1}{2}} \|_{\infty}^2}{\| s_{T,i+1} \|_{\infty}^2 + \| s_{T,i+\frac{1}{2}} \|_{\infty}^2}$$

$$\| s \|_{\infty}^2 = \max(k_0 t^2 + \frac{1}{k_0} w^2)$$

$$\boxed{\max(\eta_N; \eta_T) < \varepsilon}$$

[Ribeaucourt R., Baietto M.C., Gavouil A., CMAME 2007]

2

Stabilization of the three field weak formulation

- The X-FEM three field weak formulation can be unstable whatever the non-linear

$$\begin{bmatrix} \mathbf{K} & 0 & -\mathbf{K}_{u\lambda} \\ 0 & \mathbf{K}_{ww} & \mathbf{K}_{w\lambda} \\ -\mathbf{K}_{u\lambda}^T & \mathbf{K}_{w\lambda}^T & 0 \end{bmatrix} \begin{pmatrix} \mathbf{U}_{i+1} \\ \mathbf{W}_{i+1} \\ \Lambda_{i+1} \end{pmatrix} = \begin{pmatrix} \mathbf{F} \\ \mathbf{K}_{w\lambda} \cdot \mathbf{T}_{i+\frac{1}{2}} + \mathbf{K}_{ww} \cdot \mathbf{W}_{i+\frac{1}{2}} \\ 0 \end{pmatrix}$$

- Introduction of a stabilization term on the local-global coupling condition in order to satisfy the LBB condition:

$$\begin{bmatrix} \mathbf{K} & 0 & -\mathbf{K}_{u\lambda} \\ 0 & \mathbf{K}_{ww} & \mathbf{K}_{w\lambda} \\ -\mathbf{K}_{u\lambda}^T & \mathbf{K}_{w\lambda}^T & \boxed{\mathbf{K}_{\lambda\lambda}} \end{bmatrix} \begin{pmatrix} \mathbf{U}_{i+1} \\ \mathbf{W}_{i+1} \\ \Lambda_{i+1} \end{pmatrix} = \begin{pmatrix} \mathbf{F} \\ \mathbf{K}_{w\lambda} \cdot \mathbf{T}_{i+\frac{1}{2}} + \mathbf{K}_{ww} \cdot \mathbf{W}_{i+\frac{1}{2}} \\ \boxed{\mathbf{K}_{\lambda\lambda} \cdot \Lambda_i} \end{pmatrix}$$

→ $\begin{pmatrix} \mathbf{A} & \mathbf{B}^T \\ \mathbf{B} & -\varepsilon \mathbf{D} \end{pmatrix} \begin{pmatrix} \mathbf{Y} \\ \mathbf{Z} \end{pmatrix} = \begin{pmatrix} \mathbf{F} \\ -\varepsilon \mathbf{d} \end{pmatrix}$

The exact solution is obtained at convergence

- Stability condition of Ladyzhenskaya-Babuška-Brezzi (LBB):

$$\inf_{\mathbf{Z} \in \mathcal{Z} \setminus 0} \sup_{\mathbf{Y} \in \mathcal{Y} \setminus 0} \frac{\mathbf{Y}^T \mathbf{B}^T \mathbf{Z}}{\|\mathbf{Y}\|_{\mathcal{Y}} \cdot \|\mathbf{Z}\|_{\mathcal{Z}}} \geq \beta > 0 \quad \text{with} \quad \left\{ \begin{array}{l} \|\mathbf{Y}\|_{\mathcal{Y}} \leq \frac{1}{\alpha M_a \varepsilon + \beta^2} \cdot \|\varepsilon \mathbf{d}\| \\ \|\mathbf{Z}\|_{\mathcal{Z}} \leq \frac{4 M_a^{1/2} M_b}{2 M_a^{1/2} \alpha \varepsilon + \alpha^{1/2} \beta M_b} \cdot \|\mathbf{F}\| + \frac{4 M_a}{M_a \varepsilon + \beta^2} \cdot \|\varepsilon \mathbf{d}\| \end{array} \right.$$

2

Stabilization of the three field weak formulation – elements of

- Consider the following linear system: $\begin{pmatrix} \mathbf{A} & \mathbf{B}^T \\ \mathbf{B} & 0 \end{pmatrix} \begin{pmatrix} \mathbf{Y} \\ \mathbf{Z} \end{pmatrix} = \begin{pmatrix} \mathbf{F} \\ 0 \end{pmatrix}$
- Block condensation: $\begin{pmatrix} \mathbf{A} & \mathbf{B}^T \\ 0 & \mathbf{CS} \end{pmatrix} \begin{pmatrix} \mathbf{Y} \\ \mathbf{Z} \end{pmatrix} = \begin{pmatrix} \mathbf{F} \\ \mathbf{FS} \end{pmatrix}$
- Schur complement: $\mathbf{CS} = \mathbf{B} \mathbf{A}^{-1} \mathbf{B}^T \quad \mathbf{FS} = \mathbf{B} \mathbf{A}^{-1} \mathbf{F}$
- CS invertible if $\text{kernel}(\mathbf{B}^T) = 0$ That is to say $\max_{\mathbf{Y}} (\mathbf{B} \mathbf{Y}, \mathbf{Z}) = \max_{\mathbf{Y}} (\mathbf{Y}, \mathbf{B}^T \mathbf{Z}) > 0 \quad \forall \mathbf{Z}$
- Case of finite element: $\begin{pmatrix} \mathbf{A}_h & \mathbf{B}_h^T \\ \mathbf{B}_h & 0 \end{pmatrix} \begin{pmatrix} \mathbf{Y}_h \\ \mathbf{Z}_h \end{pmatrix} = \begin{pmatrix} \mathbf{F}_h \\ 0 \end{pmatrix} \quad \max_{\mathbf{Y}_h \in \mathcal{Y}_h} \frac{\mathbf{Y}_h^T \mathbf{B}_h^T \mathbf{Z}_h}{\|\mathbf{Y}_h\|_{\mathcal{Y}_h} \cdot \|\mathbf{Z}_h\|_{\mathcal{Z}_h}} > 0$
- When h tends to zero, one obtains the LBB condition: $\inf_{\mathbf{Z} \in \mathcal{Z} \setminus 0} \sup_{\mathbf{Y} \in \mathcal{Y} \setminus 0} \frac{\mathbf{Y}^T \mathbf{B}^T \mathbf{Z}}{\|\mathbf{Y}\|_{\mathcal{Y}} \cdot \|\mathbf{Z}\|_{\mathcal{Z}}} \geq \beta > 0$
- Error Estimator:

$$\|\mathbf{Y}_{exact} - \mathbf{Y}_h\|_1 + \|\mathbf{Z}_{exact} - \mathbf{Z}_h\|_0 \leq C_Y h^k \cdot \|\mathbf{Y}_{exact}\|_{k+1} + C_Z h^{l+1} \cdot \|\mathbf{Z}_{exact}\|_{l+1}$$

2

Stabilization of the three field weak formulation – elements of

- Consider the following linear system $\begin{pmatrix} \mathbf{A} & \mathbf{B}^T \\ \mathbf{B} & -\varepsilon \mathbf{D} \end{pmatrix} \begin{pmatrix} \mathbf{Y} \\ \mathbf{Z} \end{pmatrix} = \begin{pmatrix} \mathbf{F} \\ -\varepsilon \mathbf{d} \end{pmatrix}$

- Ellipticity condition on A:** $\alpha \|\mathbf{Y}\|_{\mathcal{Y}}^2 \leq \mathbf{Y}^T \mathbf{A} \mathbf{Y} \quad \forall \mathbf{Y} \in \mathcal{Y}$

- inf-sup condition:** there exists a positive constant β independent on the mesh (h) such that:

$$(\text{Ladyzhenskaya-Babuška-Brezzi stability condition}) \quad \inf_{\mathbf{Z} \in \mathcal{Z} \setminus 0} \sup_{\mathbf{Y} \in \mathcal{Y} \setminus 0} \frac{\mathbf{Y}^T \mathbf{B}^T \mathbf{Z}}{\|\mathbf{Y}\|_{\mathcal{Y}} \cdot \|\mathbf{Z}\|_{\mathcal{Z}}} \geq \beta > 0$$

- Continuity condition on A and B:** there exists two constants M_a and M_b independent on h such that:

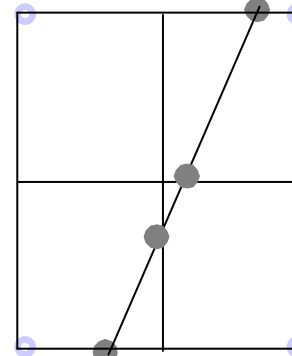
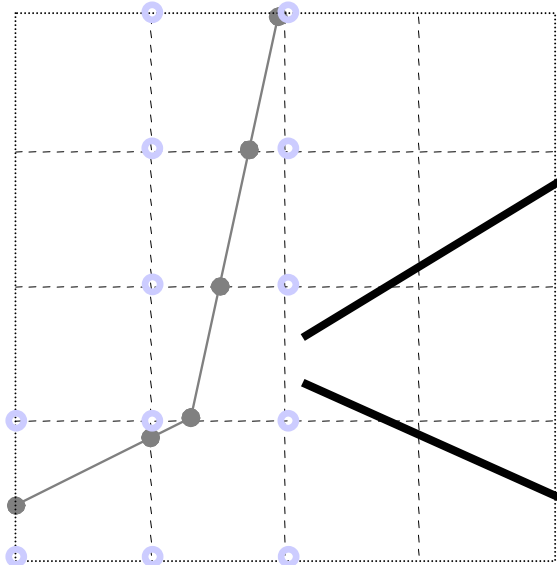
$$\begin{aligned} \forall (\mathbf{Y}, \mathbf{Z}) \in \mathcal{Y} \times \mathcal{Z} \quad \mathbf{Y}^T \mathbf{A} \mathbf{Z} &\leq M_a \|\mathbf{Y}\|_{\mathcal{Y}} \cdot \|\mathbf{Z}\|_{\mathcal{Z}} \\ \forall (\mathbf{Y}, \mathbf{Z}) \in \mathcal{Y} \times \mathcal{Z} \quad \mathbf{Y}^T \mathbf{B}^T \mathbf{Z} &\leq M_b \|\mathbf{Y}\|_{\mathcal{Y}} \cdot \|\mathbf{Z}\|_{\mathcal{Z}} \end{aligned}$$

- Property:**

$$\left\{ \begin{array}{l} \|\mathbf{Y}\|_{\mathcal{Y}} \leq \frac{1}{\alpha M_a \varepsilon + \beta^2} \cdot \|\varepsilon \mathbf{d}\| \\ \|\mathbf{Z}\|_{\mathcal{Z}} \leq \frac{4 M_a^{1/2} M_b}{2 M_a^{1/2} \alpha \varepsilon + \alpha^{1/2} \beta M_b} \cdot \|\mathbf{F}\| + \frac{4 M_a}{M_a \varepsilon + \beta^2} \cdot \|\varepsilon \mathbf{d}\| \end{array} \right.$$

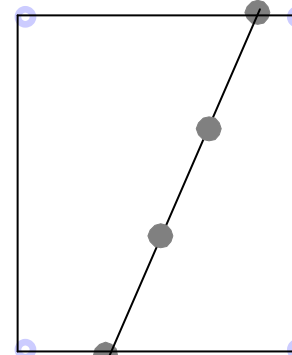
2

X-FEM discretization of the crack interface



Standard approach:
Refinement of the bulk
mesh

[Dolbow J, Moës N, Belytschko T. CMAME 2002]



New approach:
Independent
refinement

[Ladeveze 1985]
[Pierres E., Baietto M.C., Gravouil A., CMAME 2002]

- The distribution of Gauss points is the support of the primal and dual interface fields (w, t).

2

Two scales X-FEM discretization of the crack interface

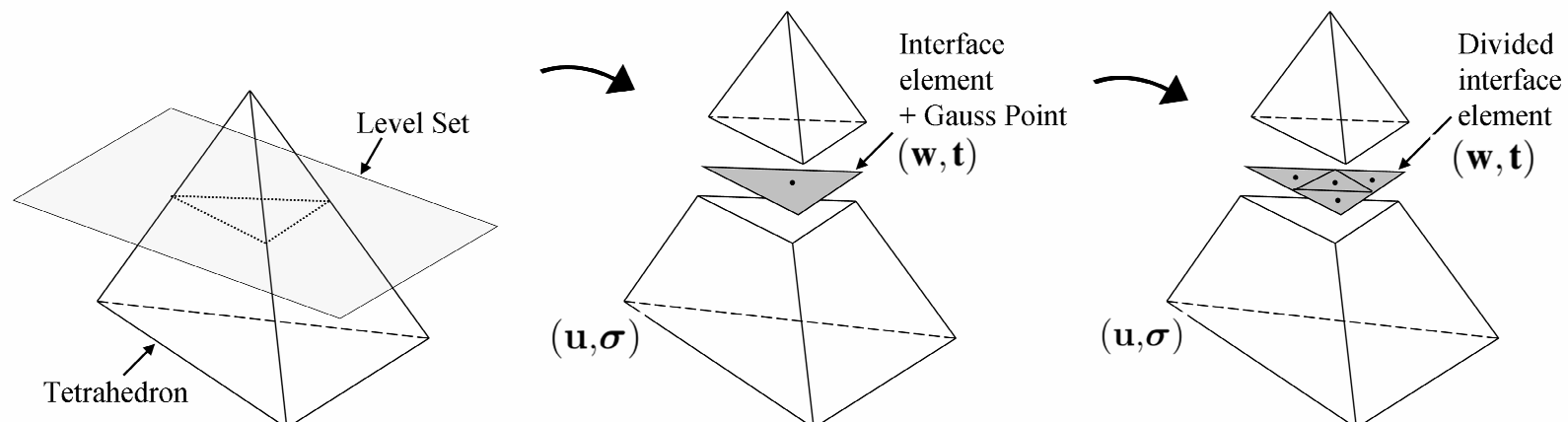
→ New approach: Independent discretization of the interface

- Discretization of the interface independent of the underlying X-FEM mesh
- Three field weak formulation: Non matching discretizations authorized

→ Interface elements divided according to size and shape.

Uniform distribution of Gauss points along the interface.

Refinement adapted to the local frictional contact

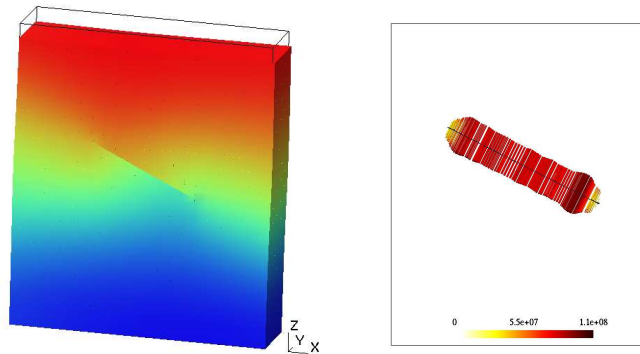


[Pierres E., Baietto M.C., Gavouil A., CMAME 2009]

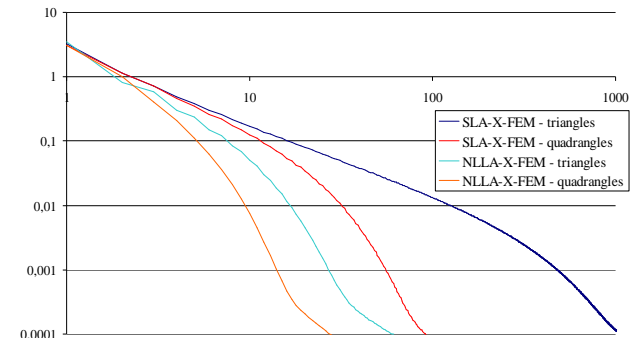
3

Efficiency and robustness of the two-scales X-FEM model for frictional cracks

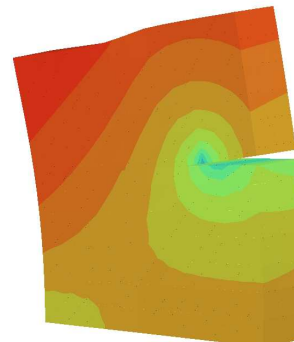
- *Numerical stability of the model*



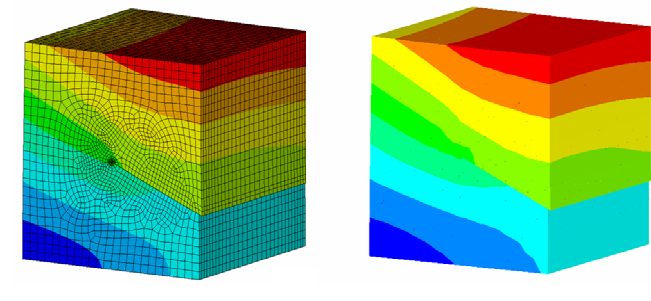
- *Non-linear convergence*



- *Accuracy and CPU saving*



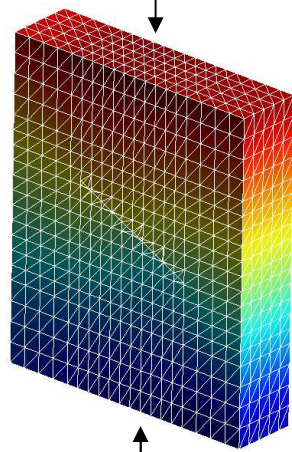
- *Efficiency of the Global-local X-FEM*



3

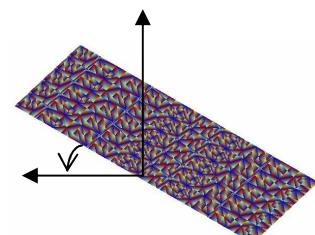
Example 1: Case of an inclined crack submitted to a compressive load

- Definition of geometry, material, crack and load



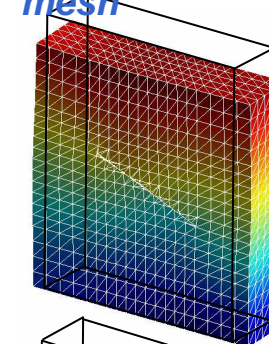
$p=100.MPa$
 $E=206.GPa$ $\nu=0.3$

- Refined interface discretization



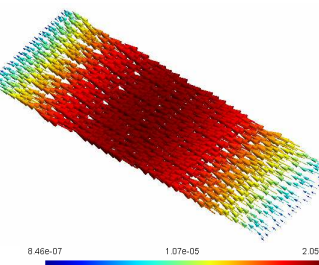
$\alpha = 30.$

Deformed mesh

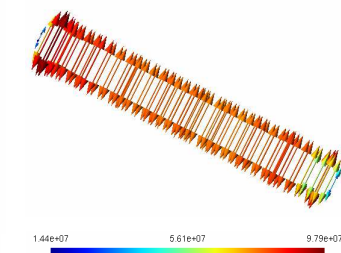


Tangential displacement field

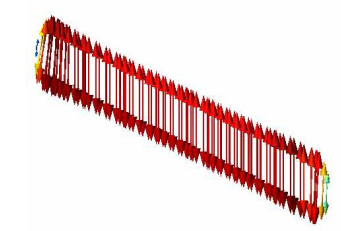
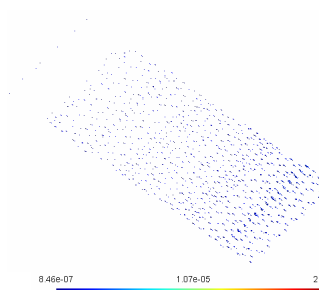
$F=0.$



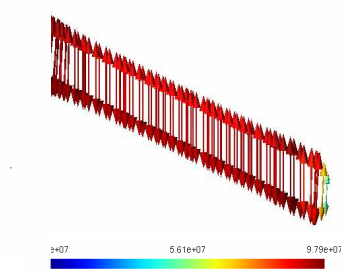
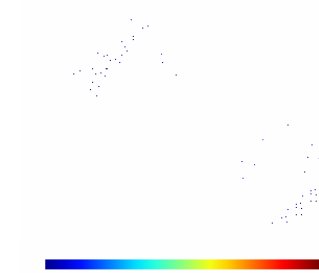
Interface load



$F=0.5$



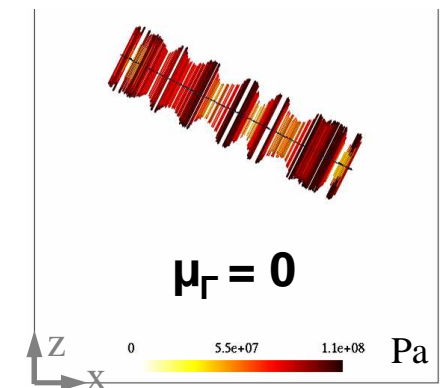
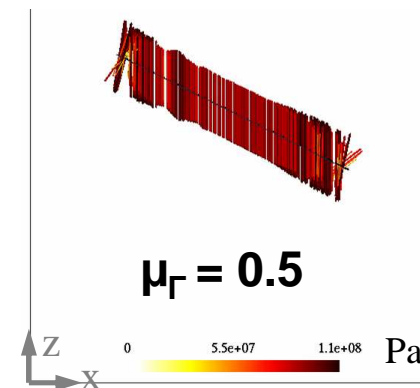
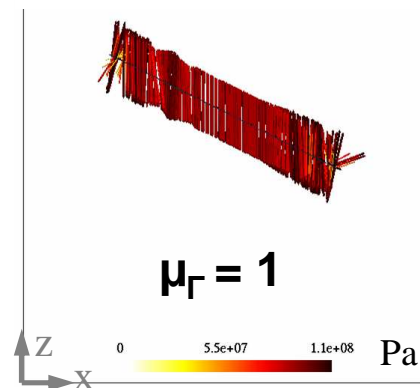
$F=1.$



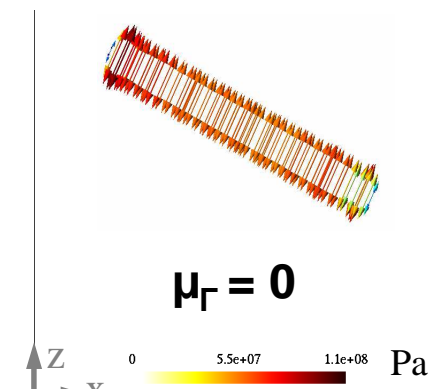
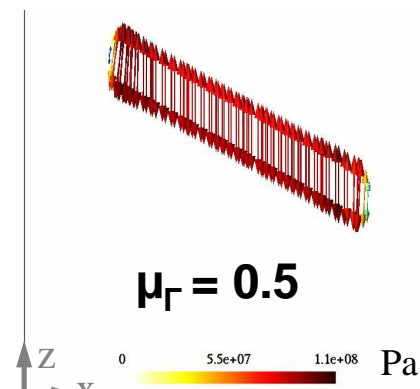
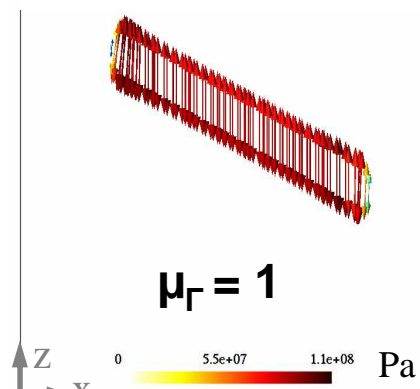
3

Stability and ability of the model to capture accurately different contact solutions

- Non stabilized model: contact load field with numerical oscillations



- Stabilized model: contact load field without numerical oscillation



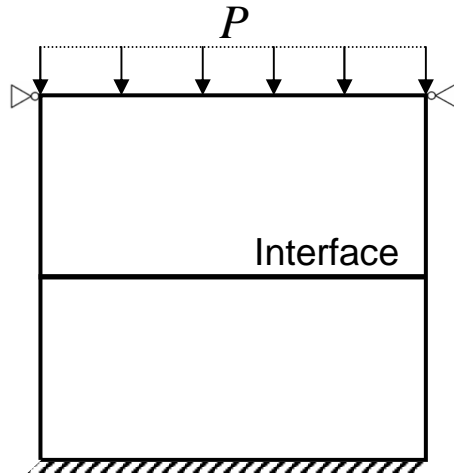
Sticking case

Partial sliding

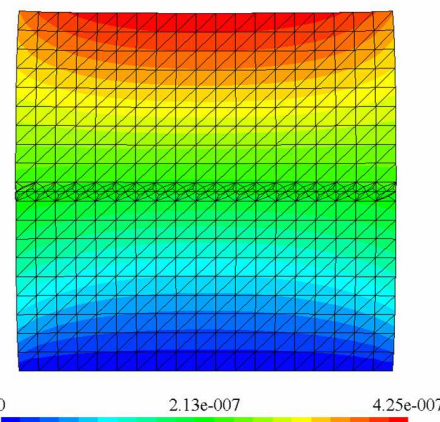
Gross sliding

3

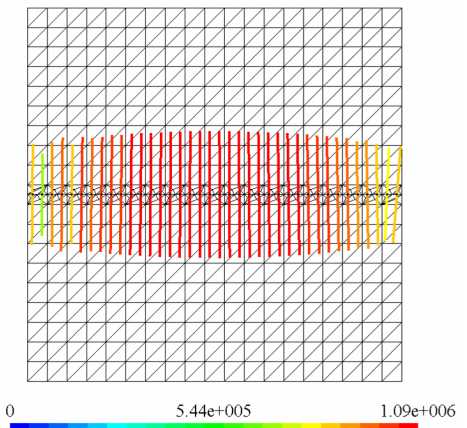
Example 2: Convergence property of the global-local X-FEM



Displacement field

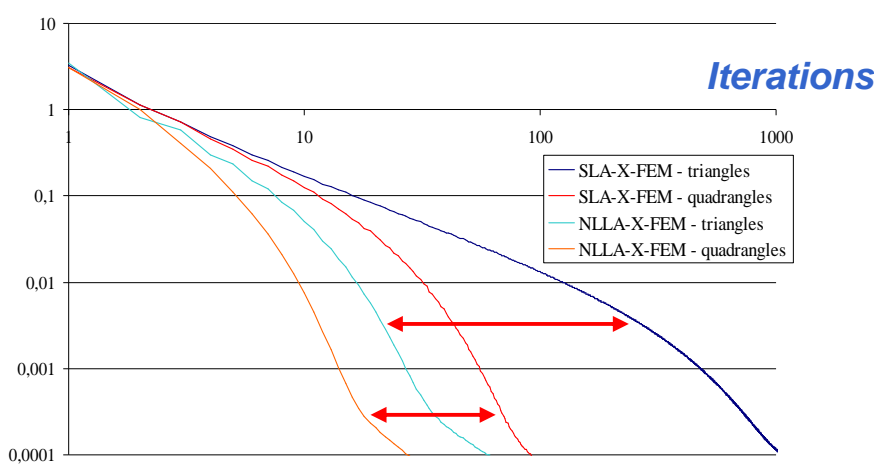


Contact loads

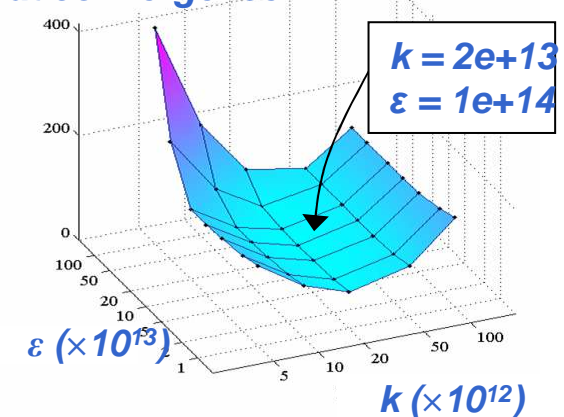


LATIN + stabilization

Local error



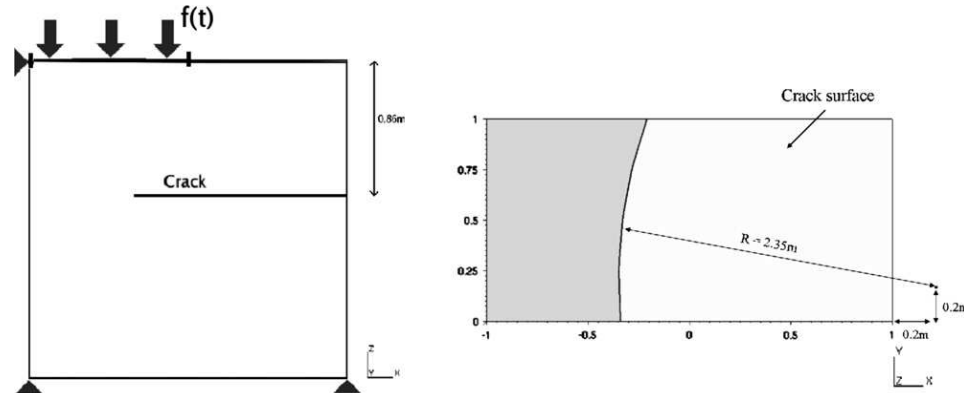
*Number of iterations
at convergence*



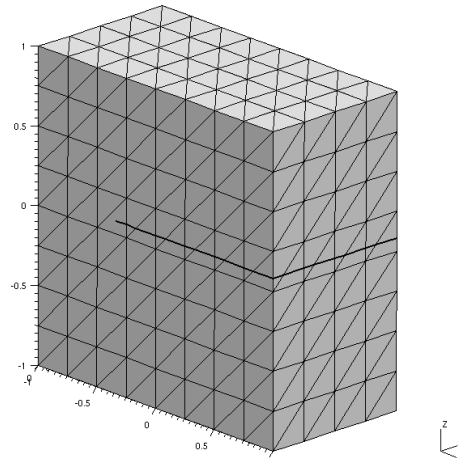
3

Example 3: A 3D crack submitted to a compressive load

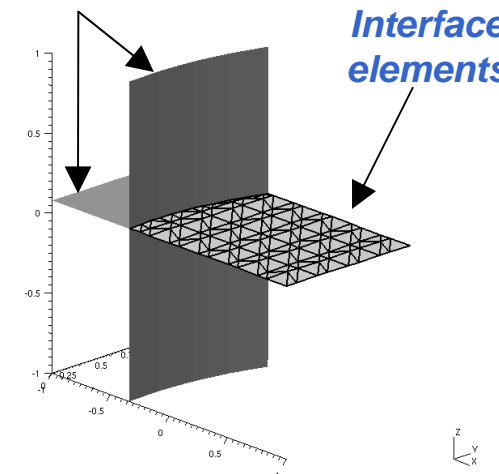
- Structure and crack geometry



- Mesh of the structure and crack:

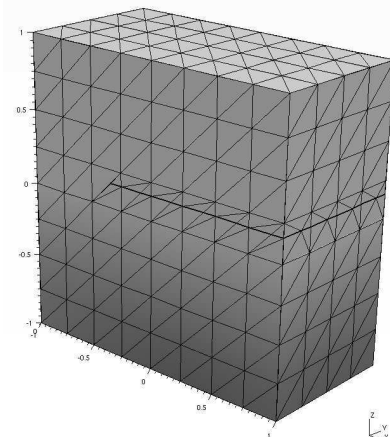


- Intersection of the crack and the X-FEM mesh
Level sets

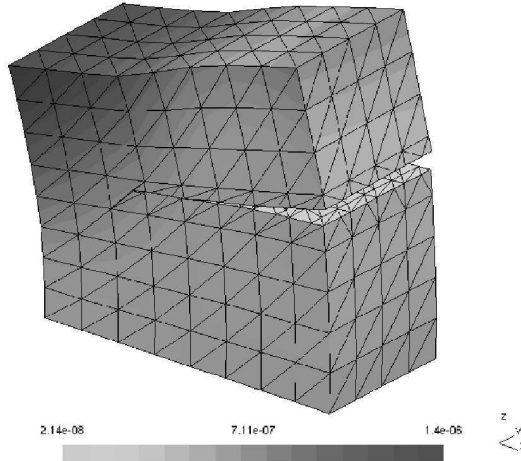


3

CASE A:

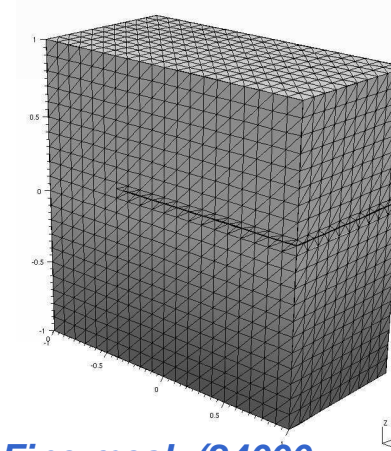


Coarse mesh (1536 elements)

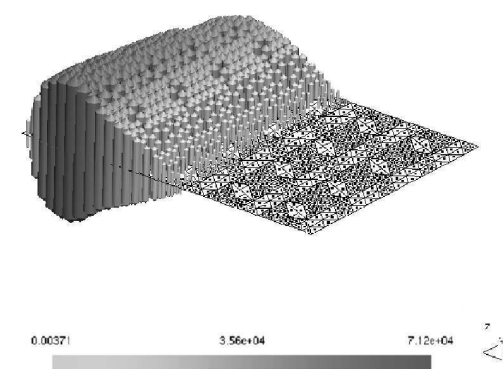


Amplified representation of the deformed mesh (case A)

CASE B:



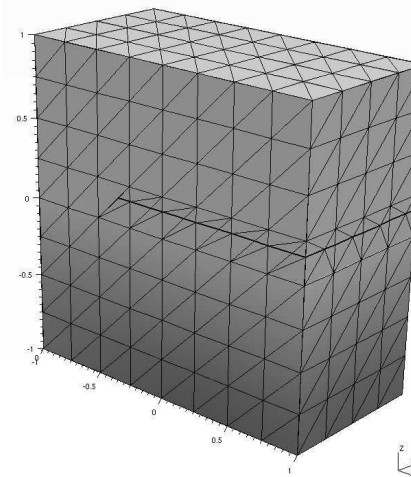
Fine mesh (24000 elements)



Three-dimensional representation of the loads along the crack interface (case B).

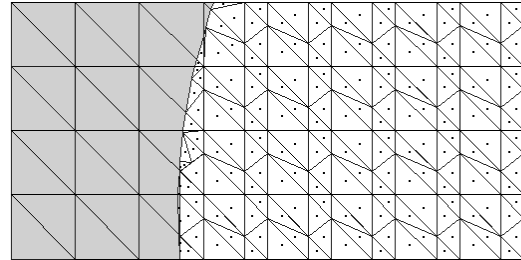
3

CASE C: Independent discretization of the interface at a given scale (recursive refinement of the Gauss points distribution at the interface)

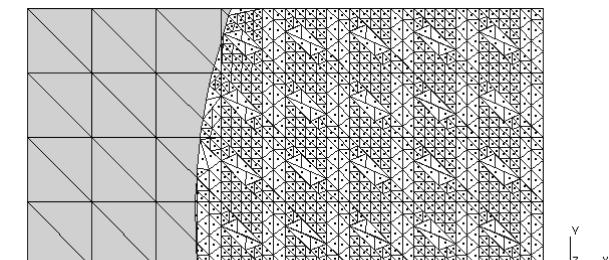


The proposed three field weak formulation authorizes non matching discretizations between the bulk and the crack

CASE A:

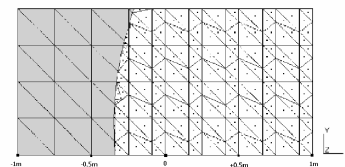


CASE C:

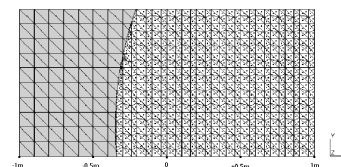


Intersection of the crack geometry and the X-FEM mesh for CASE A and CASE C

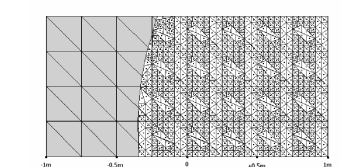
- **Case A: coarse interface discretization: 188 integration points**



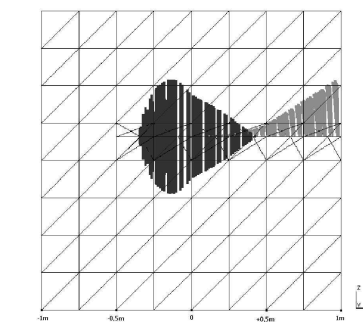
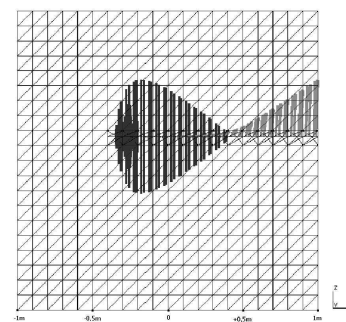
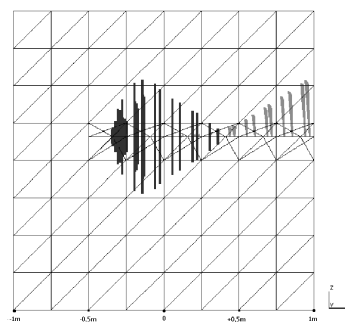
- **Case B: fine interface discretization: 1098 integration points**



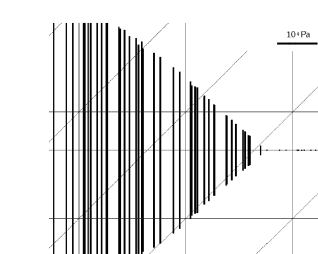
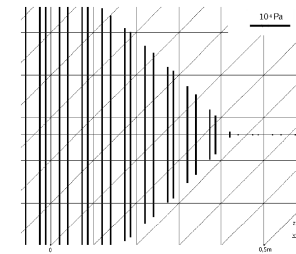
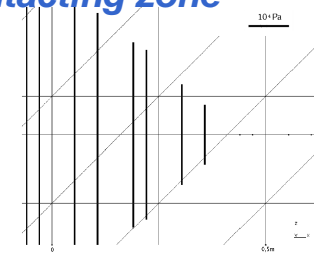
- **Case C: refined interface discretization: 1260 integration points**



- **Projection of the interface fields obtained on plane $y = 0$.**



- **View of the interfacial traction field zoomed on the transition between the open and contacting zone**



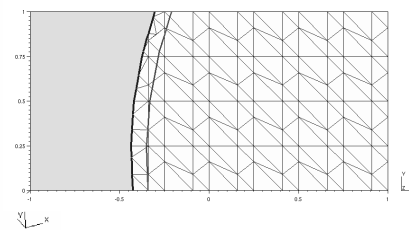
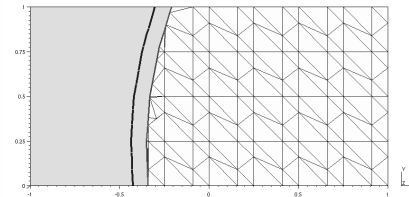
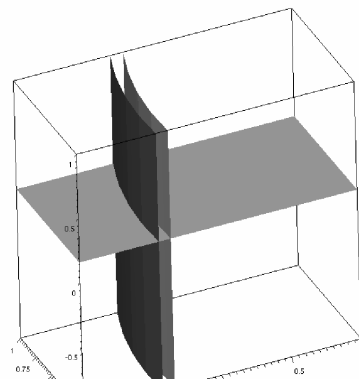
■ In both cases, the 3 field weak formulation authorizes contact discontinuities inside the 3D r

- Numerical details relative to 3D test cases A, B and C**

	Case A	Case B	Case C
3D element number	1536	24000	1536
Characteristic tetrahedron size (m)	0.25	0.1	0.25
Integration point number	188	1098	1260
Interface element size (m)	$\simeq 0.15$	$\simeq 0.06$	$\simeq 0.06$
Contact/open border location (m) and relative error along X axis, on $y = 0$ plane	0.356 7.7%	0.386 <i>ref</i>	0.399 3.3%
Relative CPU time	0.07	1	0.26

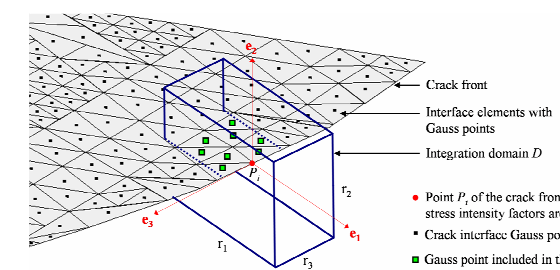
→ **70% CPU saving**

- Example of crack propagation: update of the level sets and definition of new interface elements + calculation of 3D SIFs based on 3D path independent integrals**



$$I_h = - \int_D (\sigma_{kl}^h \epsilon_{kl}^{aux} \delta_{ij} - \sigma_{kj}^h u_{k,i}^{aux} - \sigma_{kj}^{aux} u_{k,i}^h) q_{i,j} dV$$

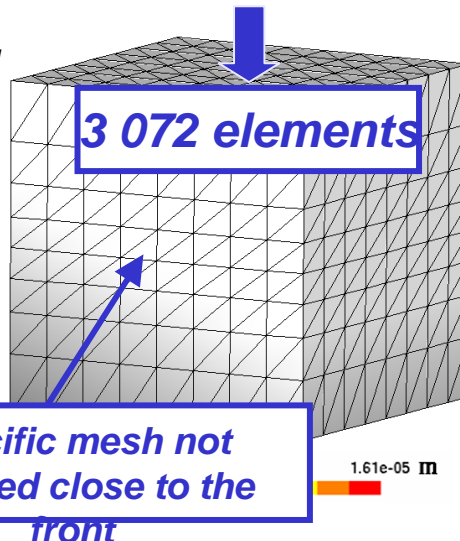
$$+ \int_{\Gamma_C^+ \cup \Gamma_C^-} (\sigma_{k2}^h u_{k,1}^{aux} + \sigma_{k2}^{aux} u_{k,1}^h) q n_C dS$$



3

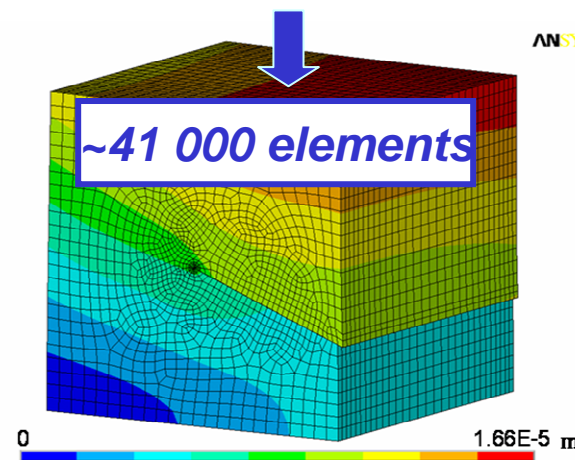
Example 4: Efficiency of the Global-local X-FEM

Global-local
X-FEM

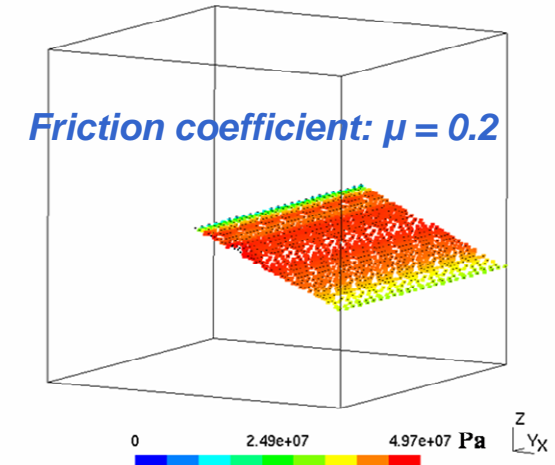


Specific mesh not
required close to the
front

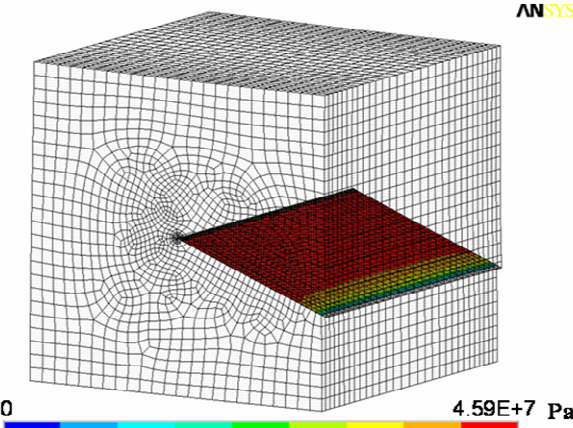
ANSYS



Displacement field



[E. Pierres et al., Tribology International
2010]



Tangential contact load

[F. Galland et al., IJNME 2010]

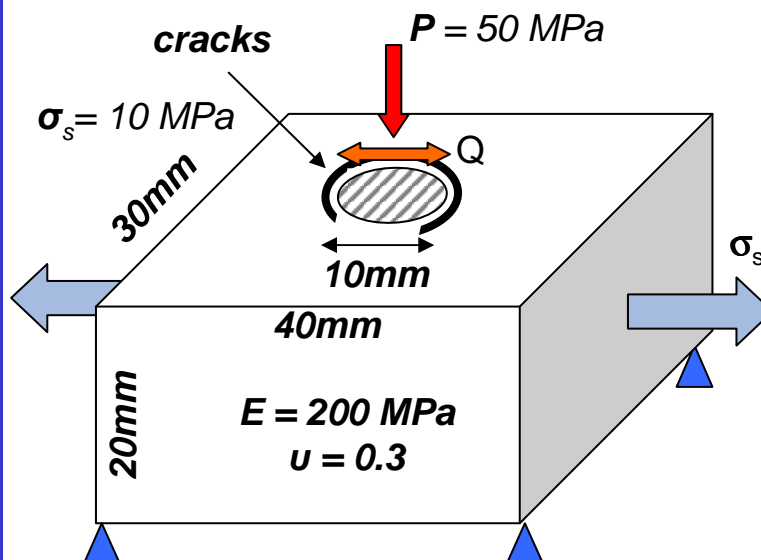
4 Numerical modeling of experimental fretting fatigue tests.



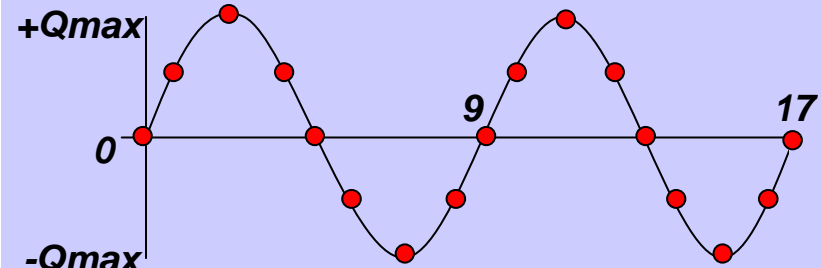
Numerical simulation with the Global – local X-FEM

[Chateauminois, Baietto, 2005]

Goal: Account for 3D complex crack geometries, local fretting loading, frictional contact conditions, multi-scale effects



Constant normal pressure $P = 50 \text{ MPa}$ and Cyclic tangential pressure $Q_{\max} = 59 \text{ MPa}$ on a circular area on the surface:



4

Multi-model strategy for the prediction of fretting crack life time

*Controlled fretting experiments
cylinder/plane or sphere/plane*



*Data loads are saved
Fretting loop: partial sliding
Calculation of the local friction coefficient $\mu(t)$*



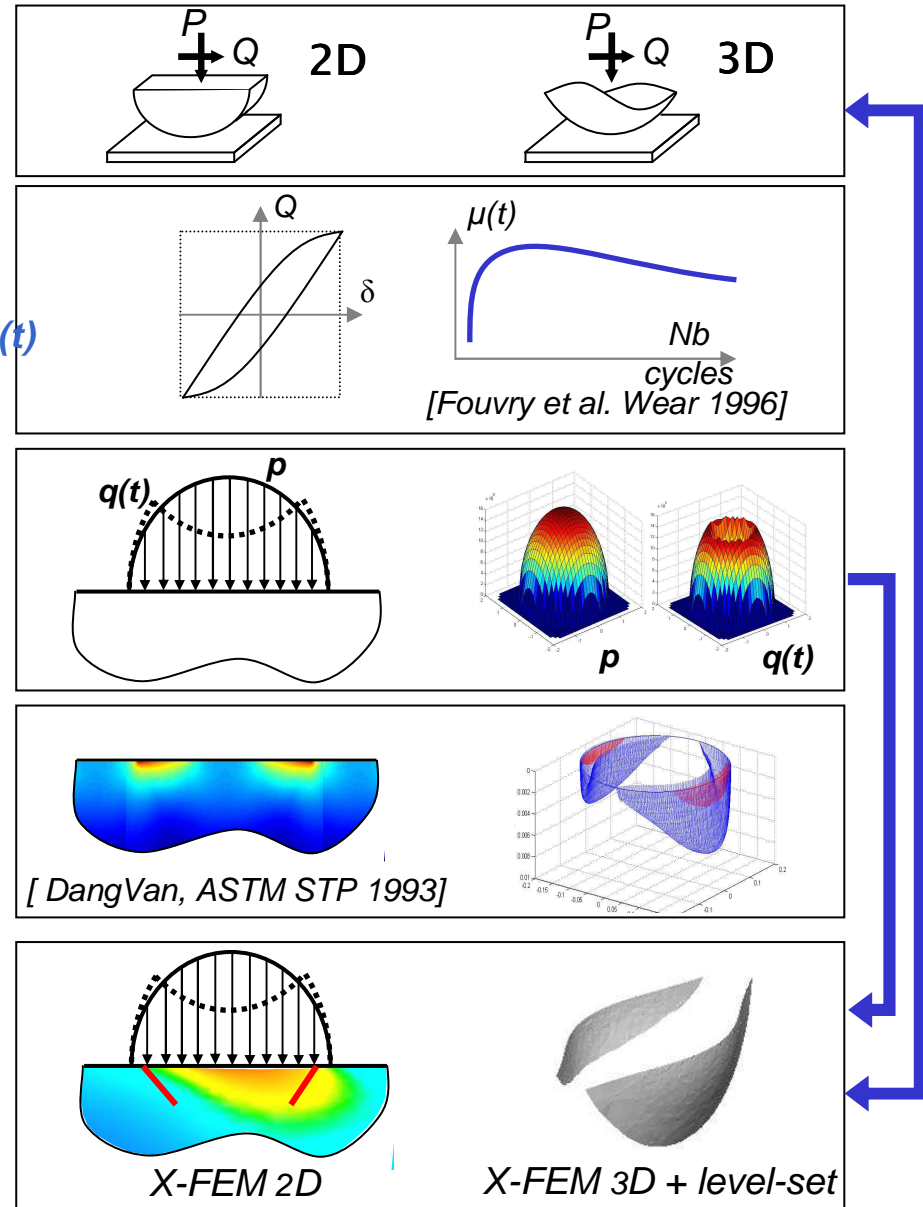
*Solving of the two-body contact pb:
Calculation of normal and tangential
stress fields (p and $q(t)$)*



*Crack initiation locations and angles:
Dang Van multi-axial fatigue criterion*



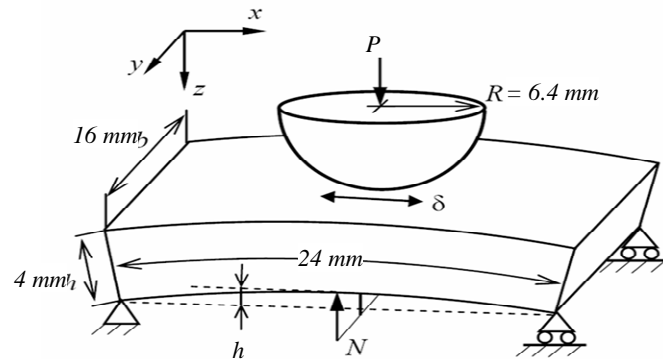
*Global - Local X-FEM
Stress Intensity Factors
2D and 3D crack propagation*



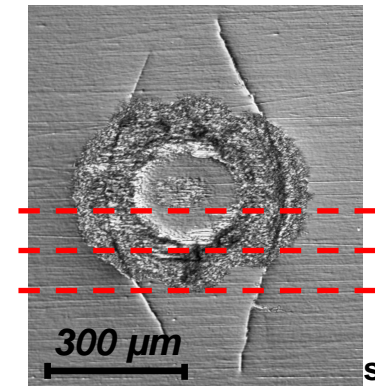
4

3D fretting fatigue experiments: sphere / plane contact (ERC SKF research center)

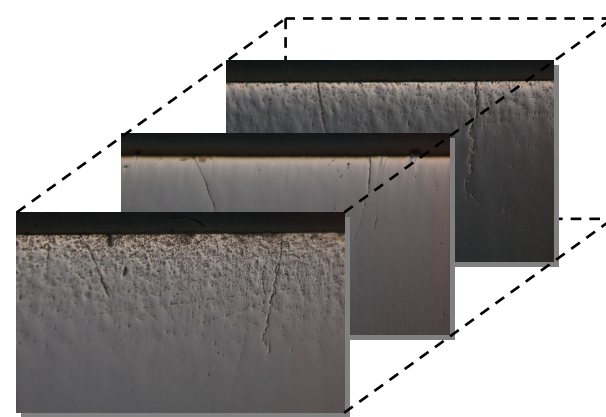
Sphere / plane experiment



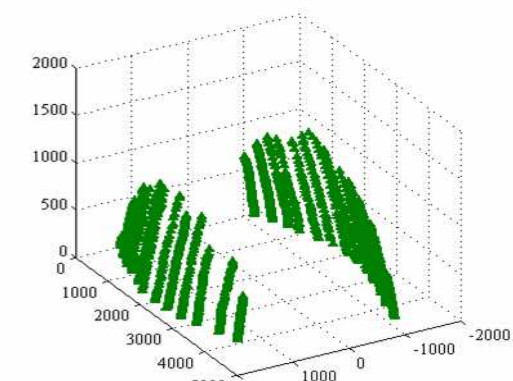
Experimental fretting crack



Transversal cut



3D crack shape reconstruction

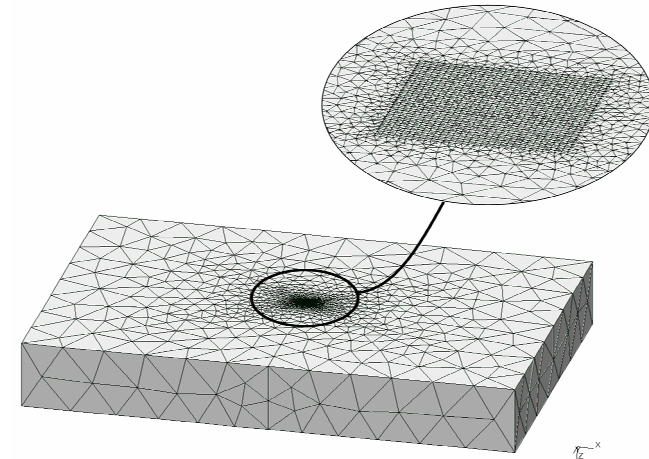


4

Global – Local X-FEM Simulation of a 3D fretting fatigue test

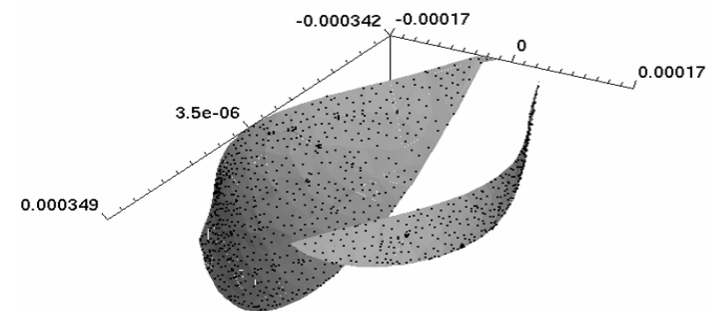
● Specimen:

- **25mm × 16mm × 4mm**
- **Steel : $E = 210 \text{ GPa}$; $\nu = 0.3$**
- **Mesh : 46266 tetraedra**
- **local refinement close to the area of interest (contact zone)**



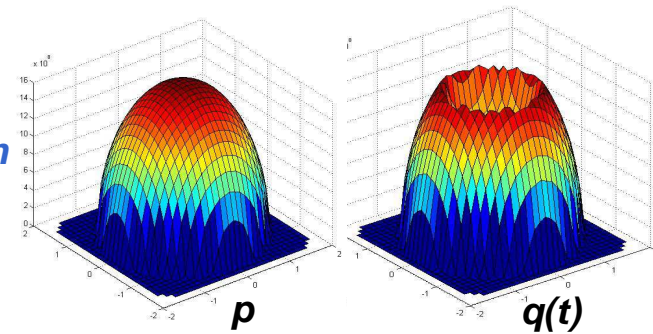
● Crack:

- **level sets**
- **Discretization: 2574 interface elements**
- **boundary crack length: ~600 μm**
- **in the bulk: ~ 100 μm**



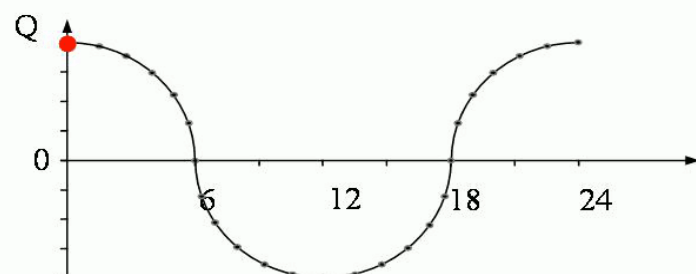
● Loading:

- **obtained from the two-body contact calculation**
- **time discretization for 1 cycle: 25 time steps**

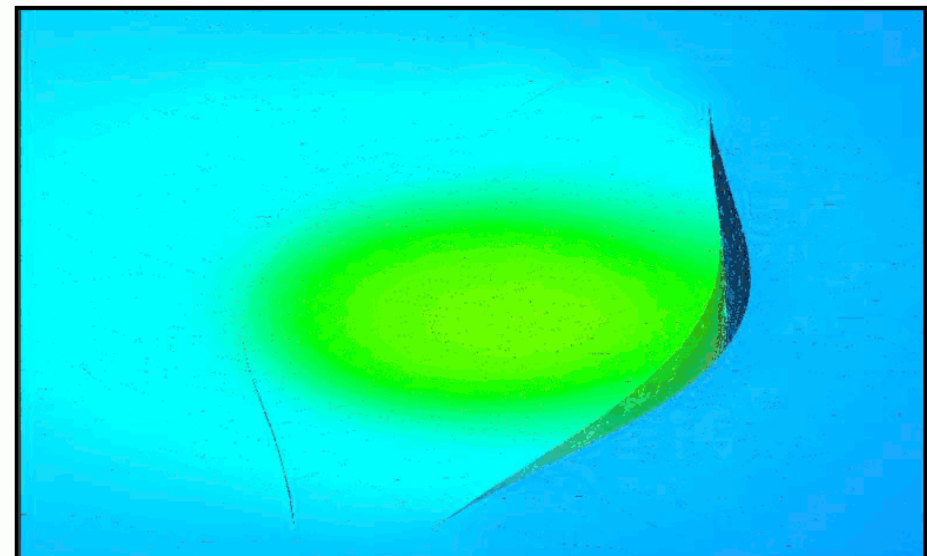


4

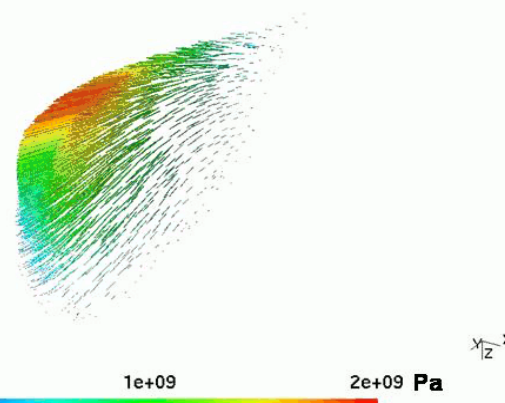
Global – Local X-FEM Simulation of a 3D fretting fatigue test



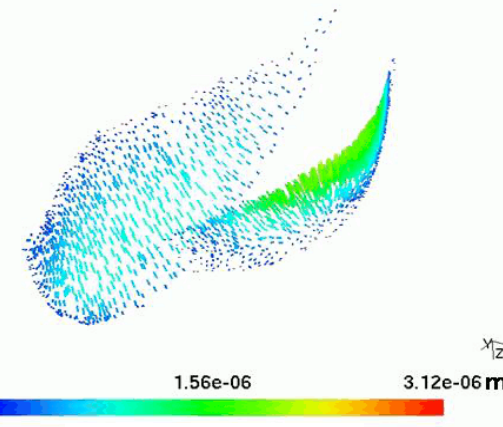
Fretting cycle



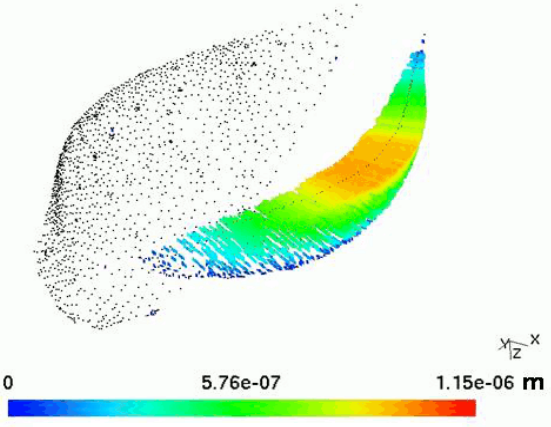
Global displacement field



contact load



Local sliding

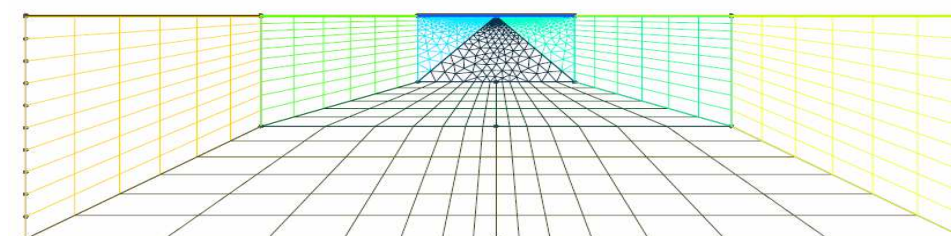
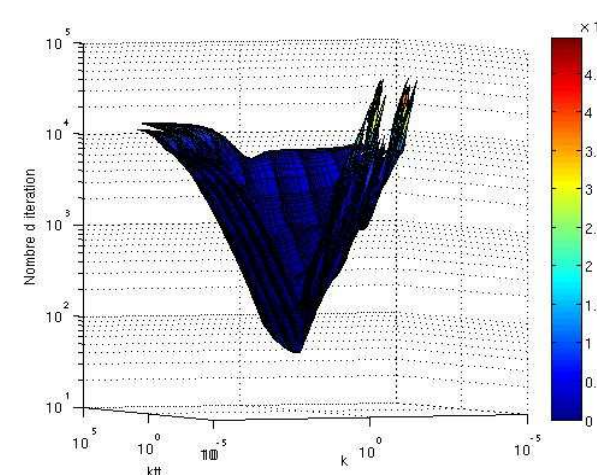


Local crack opening

4

TRAVAIL RÉALISÉ avec la SNCF: OPTIMISATION DES PERFORMANCES DU SOLVEUR X-FEM AVEC PRISE EN COMPTE DU CONTACT INTERFACIAL

- *Optimisation des performances du solveur (2 paramètres: direction de recherche, terme de stabilisation)*
- *Moins de 50 itérations NL pour un précision de 10-4*
- *Indispensable pour des problèmes en 3 dimensions*
- *Maillage multi-échelle paramétré*



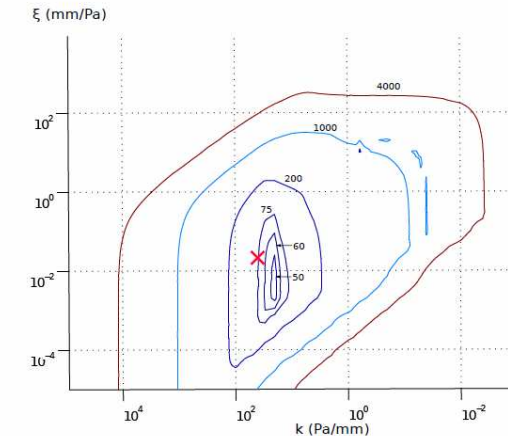
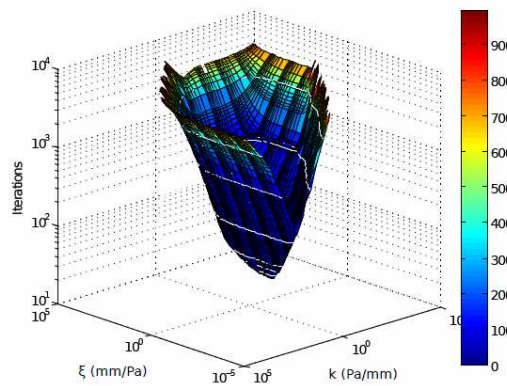
● $k = E/I$

$\xi = I/E$

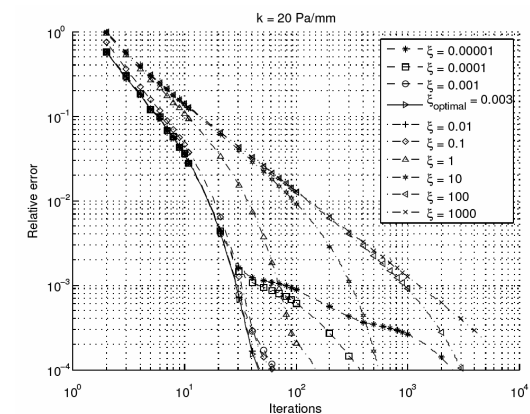
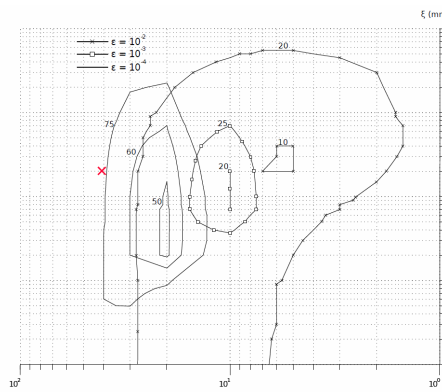
E : module de Young du matériau

I : longueur de la fissure

- *Etude de l'influence des CL, géométrie, matériau, chargement, coefficient de frottement, fissure*



- *Influence de la précision, Taux de convergence*

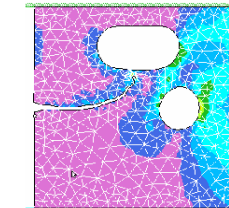
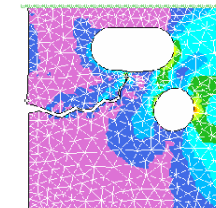
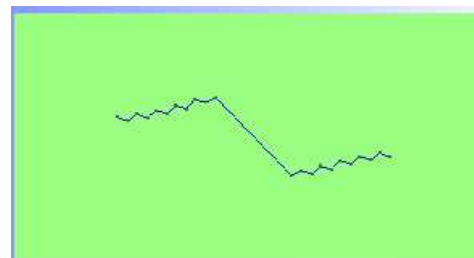


→ **Convergence plus rapide vers une solution stabilisée**

[B. Trollé, A. Gravouil, MC. Baietto, TML.Nguyen, FEAD, 2011, submitted]

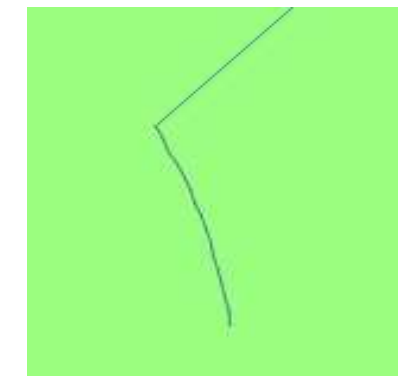
4

- TRAVAIL RÉALISÉ : MAITRISE DES ARTEFACTS NUMÉRIQUES UTILISÉE POUR SIMULER LA PROPAGATION DES FISSURES**
- *Simulation de la propagation des fissures sensible à l'erreur de discrétisation et de résolution numérique*
 - *Peu étudié sur un grand nombre de cycle*



P. O. Bouchard, CONTRIBUTION A LA MODELISATION NUMERIQUE EN MECANIQUE DE LA RUPTURE ET STRUCTURES MULTIMATERIAUX, thèse école des Mines de Paris, 2000

- *Algorithme adaptatif*



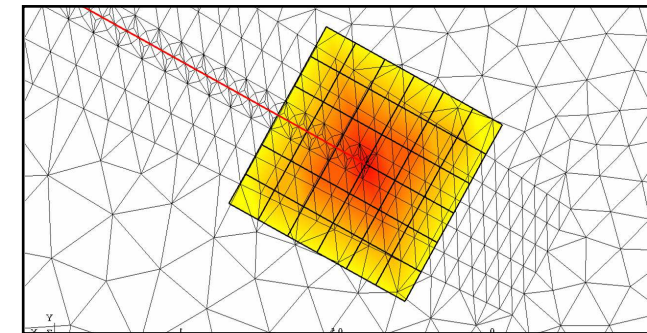
4

TRAVAIL RÉALISÉ : MAITRISE DES ARTEFACTS NUMÉRIQUES UTILISÉE POUR SIMULER LA PROPAGATION DES FISSURES

- *Stress intensity factors calculation*
2D interaction integral

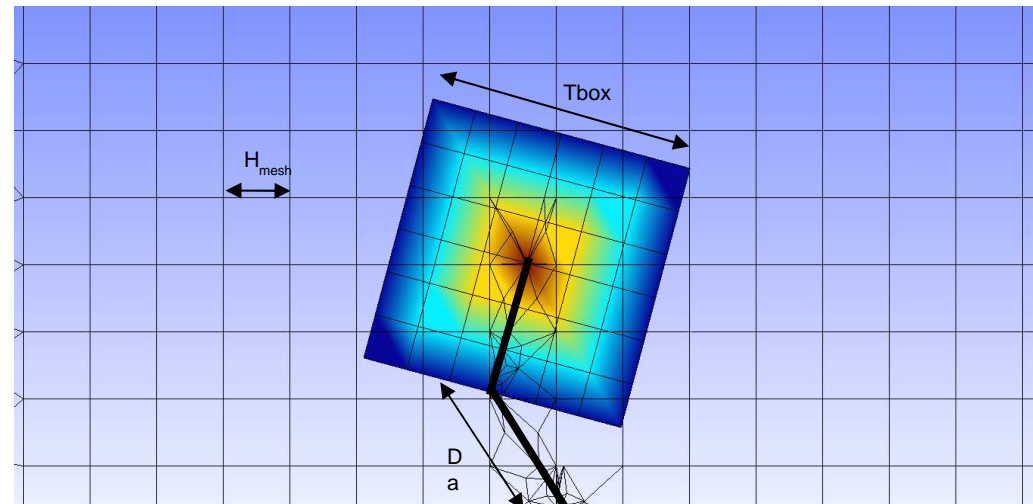
$$I^{\Re,aux} = \int_C \left(W_l^{\Re,aux} \delta_{1j} - \sigma_{ij}^{\Re} \frac{\partial u_i^{aux}}{\partial x_1} - \sigma_{ij}^{aux} \frac{\partial u_i^{\Re}}{\partial x_1} \right) n_j \, ds + \sigma_{12}^{\Re}(A) [u_1^{aux}(A)]$$

$$I^{\Re,aux} = \frac{2(1-\nu^2)}{E} \left(K_I^{\Re} K_I^{aux} + K_{II}^{\Re} K_{II}^{aux} \right)$$



Integration domain close to the crack tip

- *3 parameters for the adaptative algorithm*



4

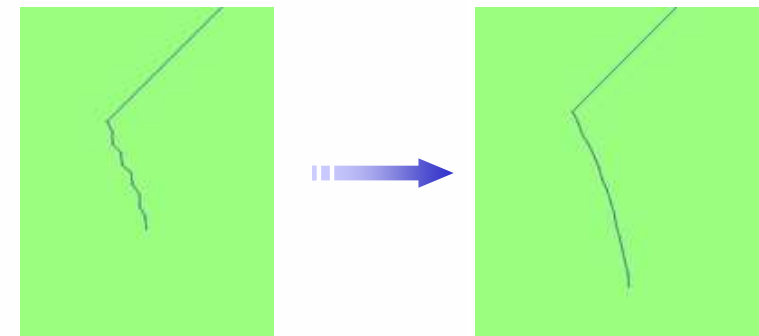
TRAVAIL RÉALISÉ : MAÎTRISE DES ARTEFACTS NUMÉRIQUES UTILISÉE POUR SIMULER LA PROPAGATION DES FISSURES

- **Algorithme 1:** Algorithme de propagation adaptatif

```

    si  $\theta_N \theta_{N-1} < 0$  et ( $\theta_N > \theta_{N-1}$  ou  $\theta_N > \theta_{coin}$ ) et  $\theta_N > \theta_{bruit}$  alors
        |  $\Delta a_N = k_{\Delta a} \Delta a_{N-1}$ 
    fin
    si  $\theta_{N-1} > \theta_{bruit}$  alors
        | si  $(N - N_{coin} - 1)\Delta a_{N-1} > 3\frac{H_{mesh}}{2}$  alors
            |   |  $Tox = 3H_{mesh}$  ou entrées utilisateurs
        fin
    sinon
        |  $Tbox = 2\Delta a_{N-1}$ 
        | si  $(\theta_{N-1} > \theta_{coin})$  alors
            |   |  $N_{coin} = N$ 
        fin
    fin
    si  $(\frac{Tbox}{2} < H_{mesh})$  alors
        |  $Tbox = H_{mesh}$ 
    fin

```



- *A erreur de discréétisation fixée, contrôle des paramètres minimisant l'erreur numérique:*

Δa variable

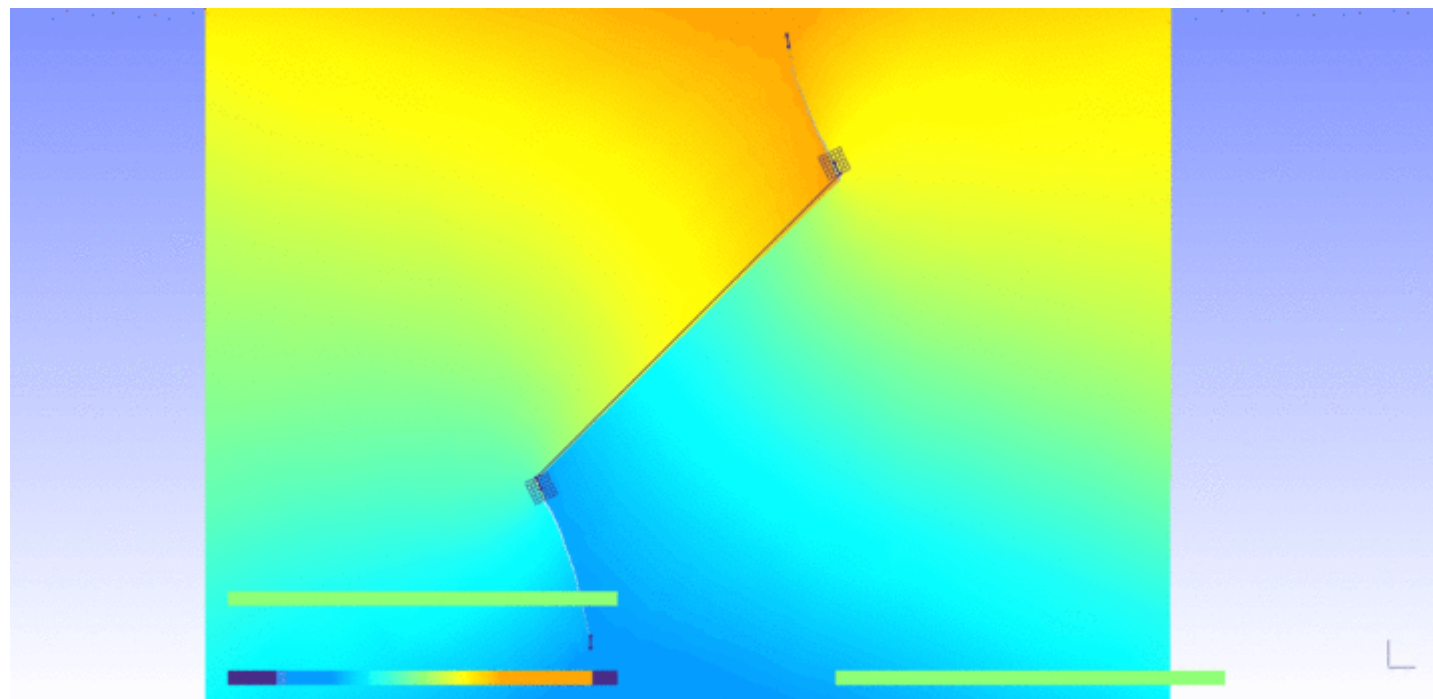
$Tbox$ s'adapte au Δa

→ *Propagation robuste avec une maîtrise de l'erreur induite par les artefacts numériques*

4

TRAVAIL RÉALISÉ : MAITRISE DES ARTEFACTS NUMÉRIQUES UTILISÉE POUR SIMULER LA PROPAGATION DES FISSURES

- *Adaptation des paramètres numériques en fonction des pas de propagation précédents*



4

LOI DE PROPAGATION EN MODE MIXTE DEDIEE À LA FATIGUE DE ROULEMENT

- *Loi du projet ICON à partir d'essai sur machine à galet*

$$\frac{da}{dn} = 2 \cdot 10^{-9} \left(\Delta K_{eq}^2 \right)^{1.665}$$

$$\Delta K_{eq}^2 = \Delta K_I^2 + 0,772 \Delta K_{II}^2$$

- *Autre loi disponible:*

$$\frac{da}{dn} = 0,000507 \left(\Delta K_{eq}^{3,74} + \Delta K_{seuil}^{3,74} \right)$$

$$\Delta K_{eq} = \sqrt{\Delta K_I^2 + \left[\left(\frac{614}{307} \right) \Delta K_{II}^{3,21} \right]^{374}}$$

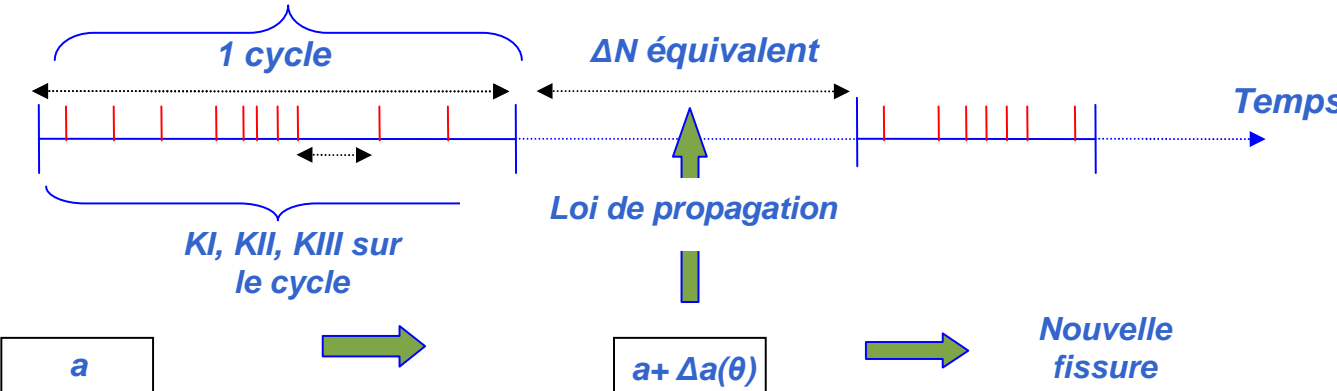
[Bold, P.; Brown, M. & Allen, R. Shear mode crack growth and rolling contact fatigue Wear, 1991, 144, 307-317]

- *Réflexion sur la mise en place d'essais de fatigue de roulement sur machine à galet LaMCoS*

4

Stratégie multi-échelle pour la simulation de la propagation des fissures

- Etape suivante : Propagation des fissures sur un grand nombre de cycle
- 2 échelles de temps :
 - Pas de temps au cours d'un cycle pour le calcul des FICs
 - Cycle entier pour la propagation
- Simulation d'un cycle discrétisé en plusieurs pas de temps

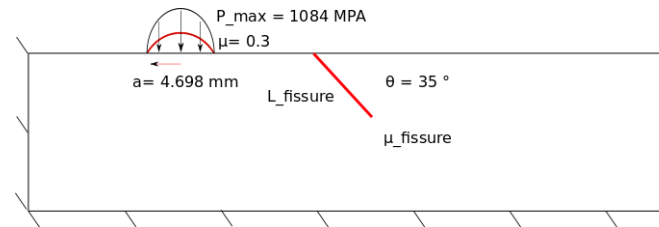


4

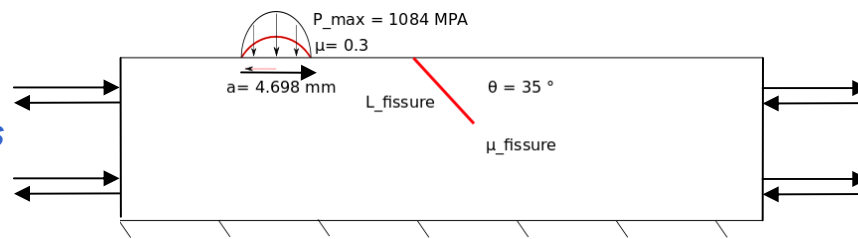
Application à la fatigue de roulement

● Première étude paramétrique

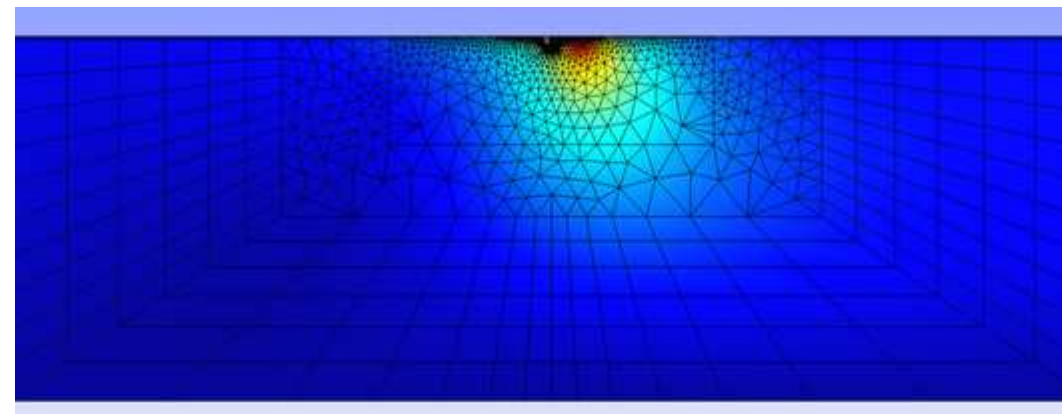
• Longueur de la fissure



• Contraintes résiduelles



Contraintes « résiduelles » : 125 MPa



4

DEVELOPPEMENT DE LA STRATEGIE SOUS CAST3M

- **Stratégie de simulation multi-échelles maîtrisée
(Logiciel dédié ELFE_3D / LaMCoS)**
- **En collaboration avec l'équipe CAST3M du CEA Saclay**
 - Assemblage de la matrice globale du système linéaire
 - Loi de Coulomb pour l'interface
 - Résolution avec la méthode LATIN
 - Indicateur spécifique au problème d'une fissure en contact frottant
- **Points durs dans l'implémentation:**
 - formulation mixte à 3 champs (solveur de l'étape globale linéaire)
 - raccord faible entre le maillage et la fissure (similaire opérateurs de maillages incompatibles)
 - XFEM avec contact + solveur LATIN

Remarque: la méthode explicite/implicite de représentation des fissures (triangulation+levelsets) développée par B P.rabel est parfaitement adaptée à une extension aux fissures frottantes dans

5

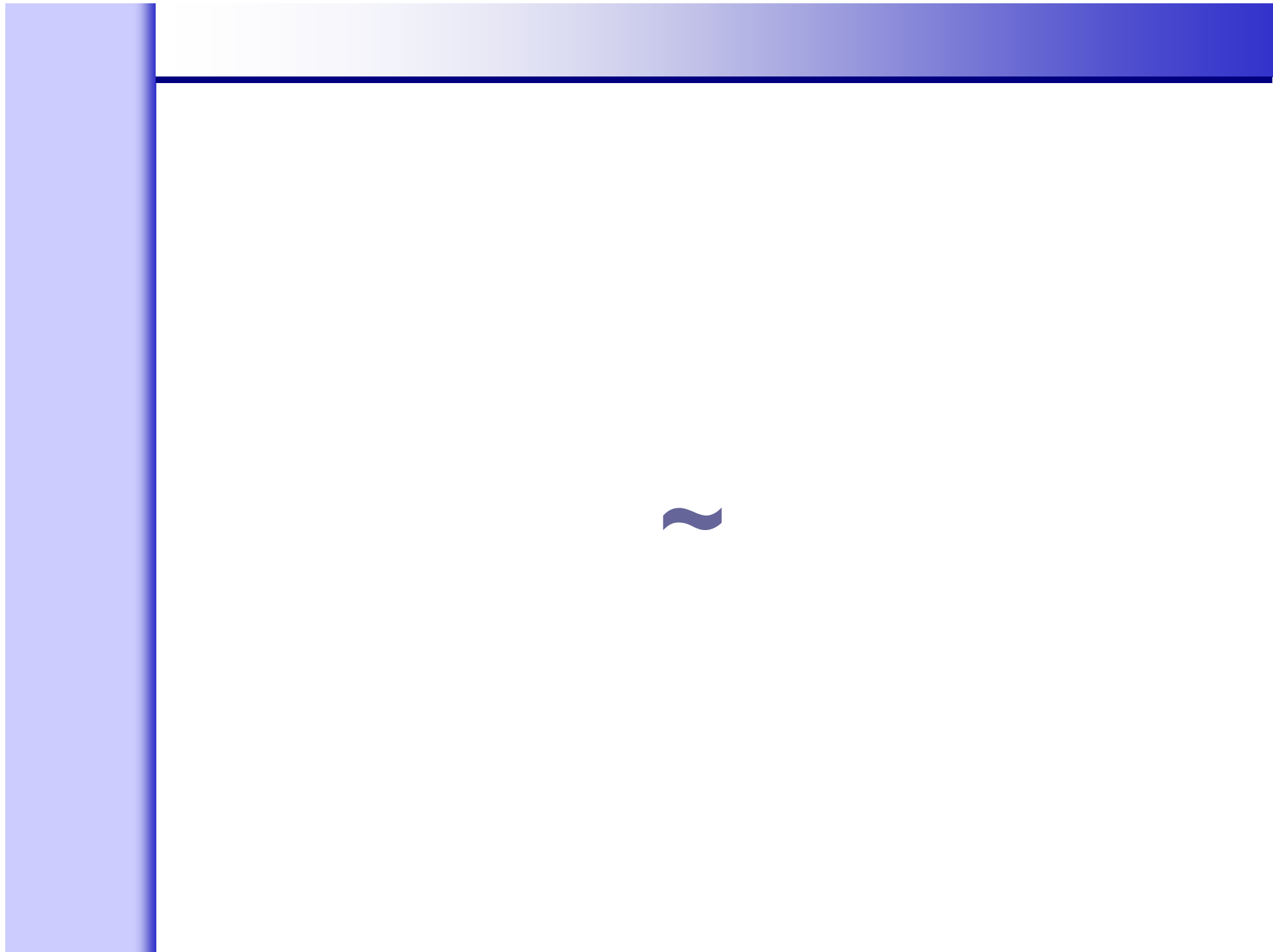
General Conclusions

- *Recovering with X-FEM a fully independence of the interface mesh from the structure mesh for contact and / or friction problems*
Describing accurately possible complex contact / friction states along the crack faces
- *The following improvements are introduced:*
 - *The crack interface is considered as an autonomous entity with its own primal and dual variables (w,t) discretization, and constitutive law (unilateral frictional coulomb's law).*
 - *An automatic refinement of the interface discretization is performed according to size and shape criteria to get a contact solution at a prescribed accuracy. It leads to a crack discretization independent from the finite element structural mesh, further adapted to the scale of interest.*
 - *An innovative three-field weak formulation coupling bulk and crack variables (u,w,t) is adopted.*

5

Contributions récentes - perspectives

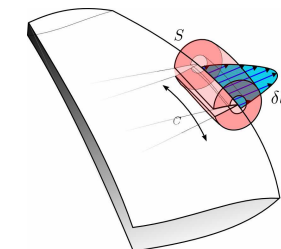
- *Optimisation du solveur X-FEM Non-linéaire avec contact / frottement*
- *Optimisation de la direction de recherche du solveur LATIN et du terme de stabilisation (moins de 50 itérations pour une précision de 10-4)*
 - *Jusqu'à un facteur 20 de gain CPU par rapport à un calcul non-optimisé (indispensable dans la perspective du 3D)*
- *Algorithme de propagation adaptatif permet une propagation où l'erreur numérique est maîtrisée (liée au maillage, au pas et à l'angle de l'incrément de propagation)*
- *Implémentation de la méthode dans CAST3M (CEA)*
- *Implémentation d'une loi de propagation en fatigue de roulement (essais de validation éventuels)*



Stress Intensity Factors calculation

- Dissipated energy for a virtual crack extension

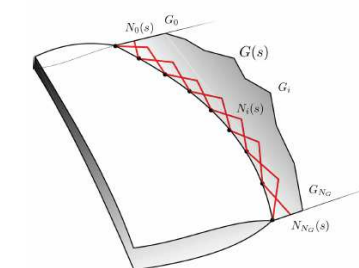
$$\int \sigma () () \quad \int \int () ()$$



- $G(s)$ is discretized along the front with curvilinear shape functions:

$$() \sum () - \int () ()$$

[Parks et al., 2000]

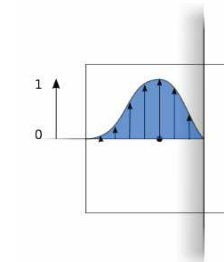


- Diagonal matrix:

$$\sum \int \sum () () = \int ()$$

- Irwin formula

$$-[() ()] - ()$$



- Interaction integral

$$\int [() ()]$$

- Contact, friction, plasticity, dynamics

$$\int () \quad \int () \quad (--)$$

[Combescure, Suo, 1986] [Moës N., Gravouil A., Belytschko T., IJNME 2002]

[Gosz & al. 1997, 2002, Béchet 2005, Réthoné 2005, Elguedj 2006, Ribeaucourt 2006]

Augmented Lagrangian Iterative Solver

- *Iterative strategy similar to LATIN method*
- *Regularization of the 3 field weak formulation by penalty terms
(influence on the convergence rate)*

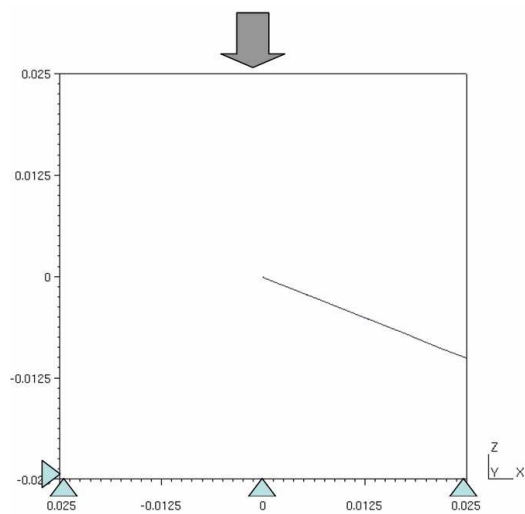
$$\begin{aligned} 0 &= - \int_{\Omega} \boldsymbol{\sigma}_{i+1} : \boldsymbol{\epsilon}(\mathbf{u}^*) d\Omega + \int_{\Gamma^t} \mathbf{f}_t \cdot \mathbf{u}^* dS + \int_{\Gamma_C} \boldsymbol{\lambda}_{i+1} \cdot \mathbf{u}^* dS \\ &\quad + \int_{\Gamma_C} (\mathbf{t}_i + \boldsymbol{\alpha} \mathbf{w}_i) \cdot \mathbf{w}^* dS - \int_{\Gamma_C} (\boldsymbol{\lambda}_{i+1} + \boldsymbol{\alpha} \mathbf{w}_{i+1}) \cdot \mathbf{w}^* dS \\ &\quad + \int_{\Gamma_C} (\mathbf{u}_{i+1} - \mathbf{w}_{i+1}) \cdot \boldsymbol{\lambda}^* dS \quad \forall \mathbf{u}^* \in U_0^*, \quad \forall \mathbf{w}^* \in W^* \text{ and } \forall \boldsymbol{\lambda}^* \in \Lambda^* \end{aligned}$$

- *Discretized formulation:*

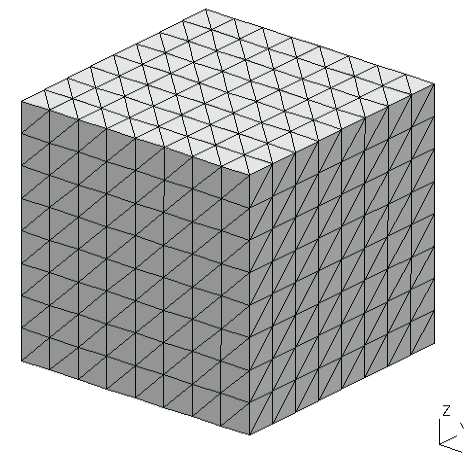
$$\begin{bmatrix} \mathbf{K} & 0 & -\mathbf{K}_{u\lambda} \\ 0 & \mathbf{K}_{ww} & \mathbf{K}_{w\lambda} \\ -\mathbf{K}_{u\lambda}^T & \mathbf{K}_{w\lambda}^T & 0 \end{bmatrix} \begin{pmatrix} \Delta \mathbf{U}_{i+1} \\ \Delta \mathbf{W}_{i+1} \\ \Delta \boldsymbol{\Lambda}_{i+1} \end{pmatrix} = \begin{pmatrix} \mathbf{F}_t + \mathbf{K}_{u\lambda} \cdot \boldsymbol{\Lambda}_i \\ \mathbf{K}_{w\lambda} \cdot (\mathbf{T}_i - \boldsymbol{\Lambda}_i) \\ \mathbf{K}_{u\lambda}^T \cdot \mathbf{U}_i - \mathbf{K}_{w\lambda}^T \cdot \mathbf{W}_i \end{pmatrix}$$

$$\begin{cases} \mathbf{u}_{i+1} = \Delta \mathbf{u}_{i+1} + \mathbf{u}_i \\ \mathbf{w}_{i+1} = \Delta \mathbf{w}_{i+1} + \mathbf{w}_i \\ \boldsymbol{\Lambda}_{i+1} = \Delta \boldsymbol{\Lambda}_{i+1} + \boldsymbol{\Lambda}_i \end{cases}$$

Validation of the model: Crack submitted to frictional contact

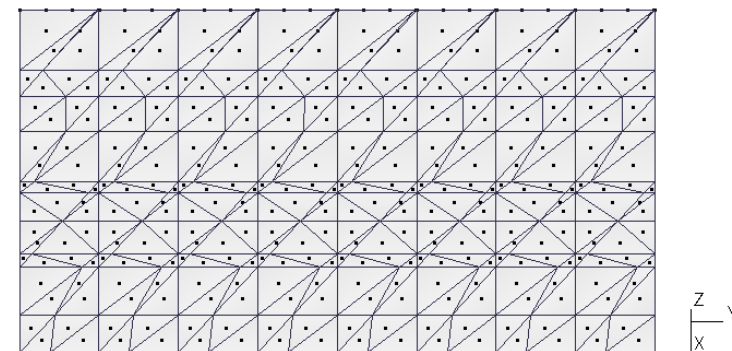


Geometry: (50mm; 50mm; 50mm)
Material: $E = 200 \text{ GPa}$, $\nu = 0,3$
Compressive pressure: 50 MPa

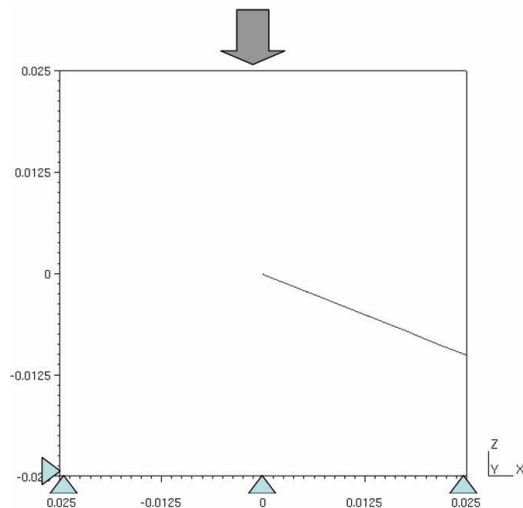


Bulk mesh:
3072 tetrahedra

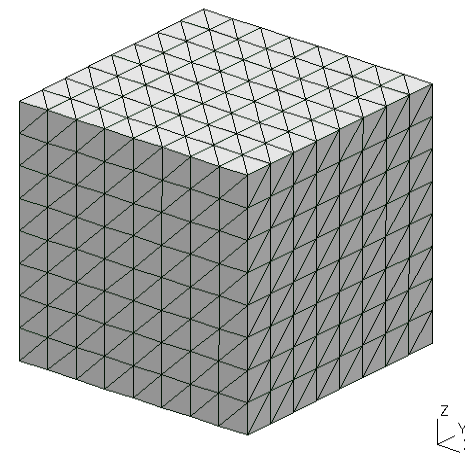
Standard interface: 360 interface elements



Validation of the model: Crack submitted to frictional contact

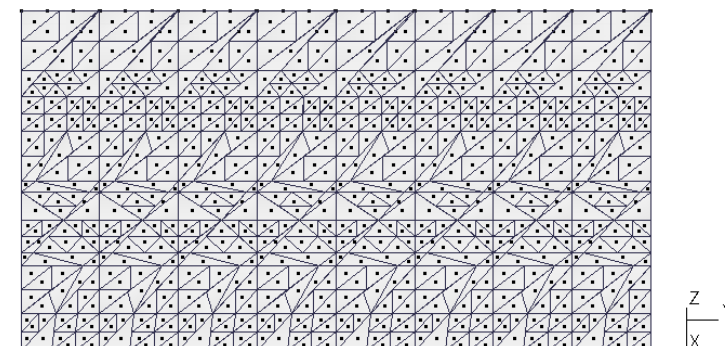


Geometry: (50mm; 50mm; 50mm)
Material: $E = 200 \text{ GPa}$, $\nu = 0,3$
Compressive pressure: 50 MPa



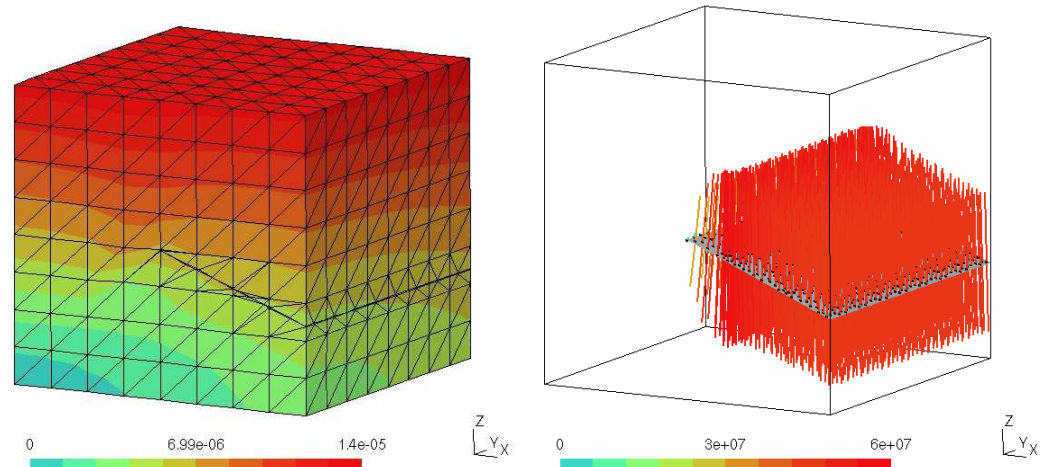
Bulk mesh:
3072 tetrahedra

Refined interface: 832 interface elements

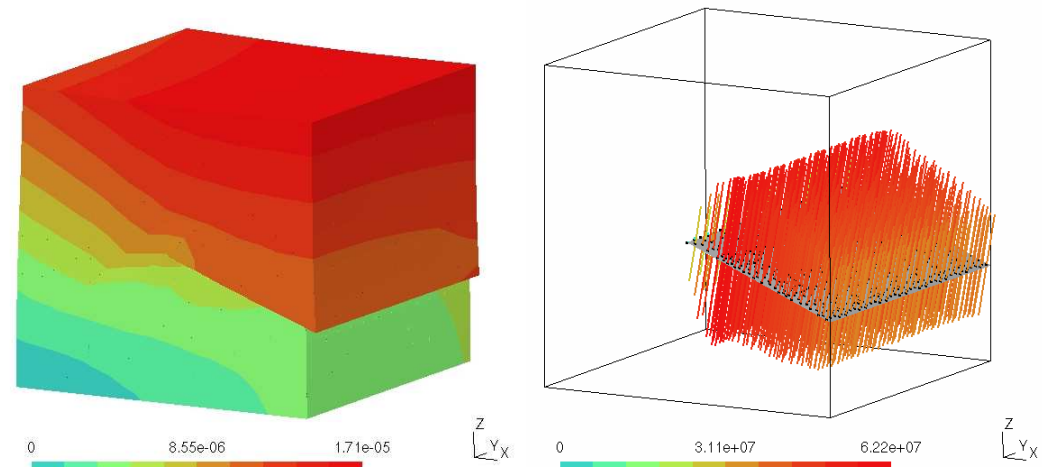


Validation of the model: Crack submitted to frictional contact

*Sticking case: $\mu = 1$
Solution very close to
uncracked body submitted
to the same loading*

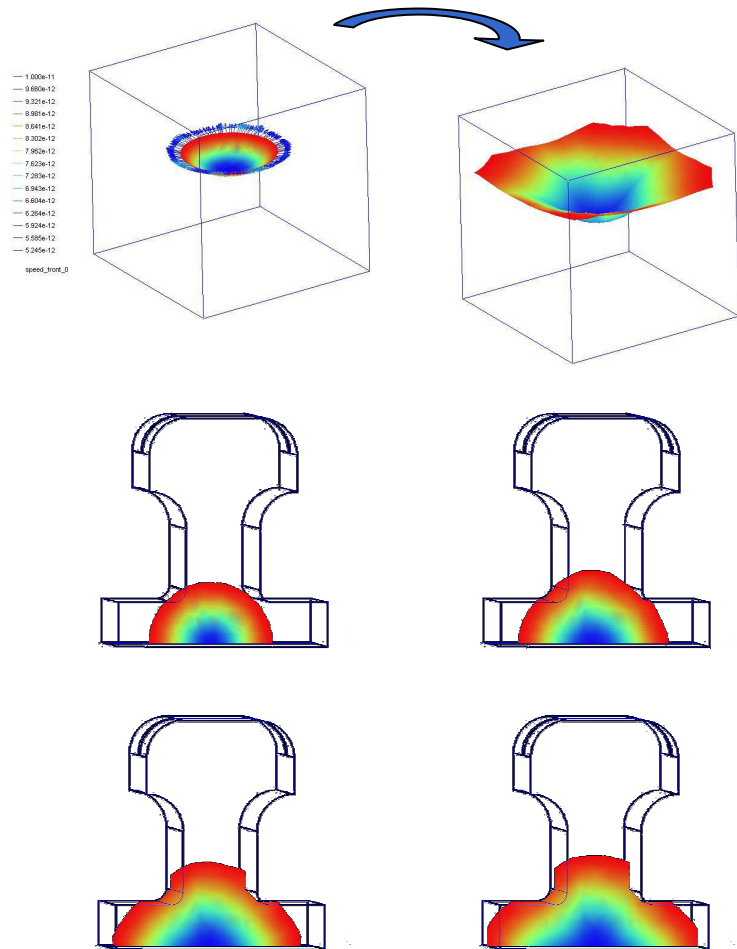


*Sliding case: $\mu = 0.2$
Good agreement with FEM
(ANSYS)*

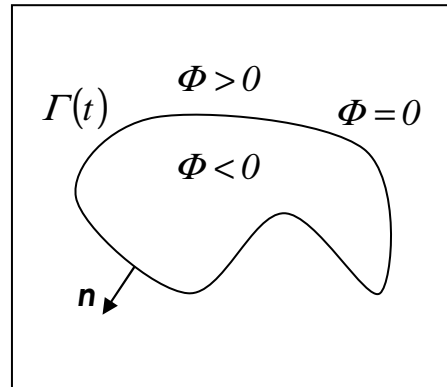


X-FEM + Level sets

- eXtended Finite Element Method + level sets
- Advantages:
 - Similar to FEM
 - No remeshing
 - No field interpolation
 - Good topologic properties
 - Flexibility in the initialization of level sets
- Drawbacks:
 - Specific numerical integration and preconditioning
 - Post-treatment
 - Specific strategies of enrichment for time-dependent problems



Level sets



Signed distance:

$$\begin{cases} \Phi(\mathbf{x}, t) < 0 & \text{in } \Omega^-(t) \\ \Phi(\mathbf{x}, t) = 0 & \text{on } \Gamma(t) \\ \Phi(\mathbf{x}, t) > 0 & \text{in } \Omega^+(t) \end{cases}$$

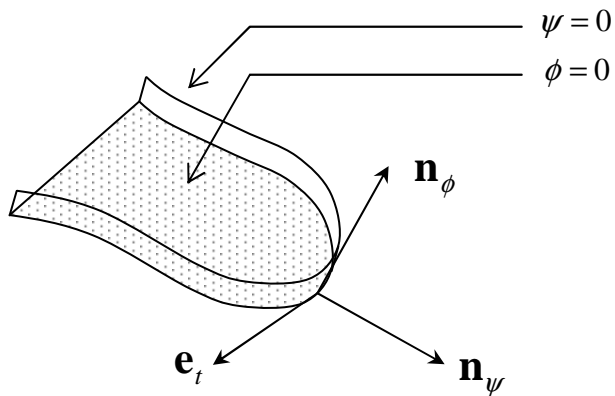
Allows to model implicitly moving interfaces

- **Governing equation:** $\frac{\partial \Phi}{\partial t} + V|\nabla \Phi| = 0$
- **Normal vector:** $\mathbf{n} = \frac{\nabla \Phi}{|\nabla \Phi|}$ **curvature:** $\kappa = \nabla \cdot \frac{\nabla \Phi}{|\nabla \Phi|}$
- **Hausdorff measure:** $|\Gamma(t)| = \int \delta(\Phi) |\nabla \Phi| dx$
- **Lebesgue measure:** $|\Omega^-(t)| = \int H(-\Phi) dx$

[Osher and Sethian 1988]

Non-planar crack modeling

- *Local basis linked to the level sets*



$$\mathbf{n}_\psi = \nabla \psi$$

$$\mathbf{n}_\phi = \nabla \phi$$

$$\mathbf{e}_t = \mathbf{n}_\psi \times \mathbf{n}_\phi$$

- *Component velocity on the local basis of the crack front V_ϕ , V_ψ and*

$$\mathbf{V} = V_\psi \mathbf{n}_\psi + V_\phi \mathbf{n}_\phi$$

Non-planar crack modeling

- *Time and space discretization for structured meshes*

$$\phi_{ij}^{n+1} = \phi_{ij}^n - \Delta t \left\{ \begin{array}{l} \left(s_{ij} n_{ij}^x \right)^+ \frac{\phi_{ij} - \phi_{i-1j}}{\Delta x} + \left(s_{ij} n_{ij}^x \right)^- \frac{\phi_{i+1j} - \phi_{ij}}{\Delta x} \\ + \left(s_{ij} n_{ij}^y \right)^+ \frac{\phi_{ij} - \phi_{ij-1}}{\Delta y} + \left(s_{ij} n_{ij}^y \right)^- \frac{\phi_{ij+1} - \phi_{ij}}{\Delta y} \end{array} \right\}$$
$$\left\{ \begin{array}{l} \tilde{\Phi}^{n+1} = \Phi^n - \Delta t H(\Phi^n) \\ \Phi^{n+1} = \frac{(\Phi^n + \tilde{\Phi}^{n+1})}{2} - \frac{\Delta t}{2} H(\tilde{\Phi}^{n+1}) \end{array} \right.$$
$$(x)^+ = \max(x, 0) \quad (x)^- = \min(x, 0) \quad s_{ij} = \frac{\Phi_{ij}}{\sqrt{\Phi_{ij}^2 + \Delta x^2}}$$

- *Time and space discretization for non-structured meshes*

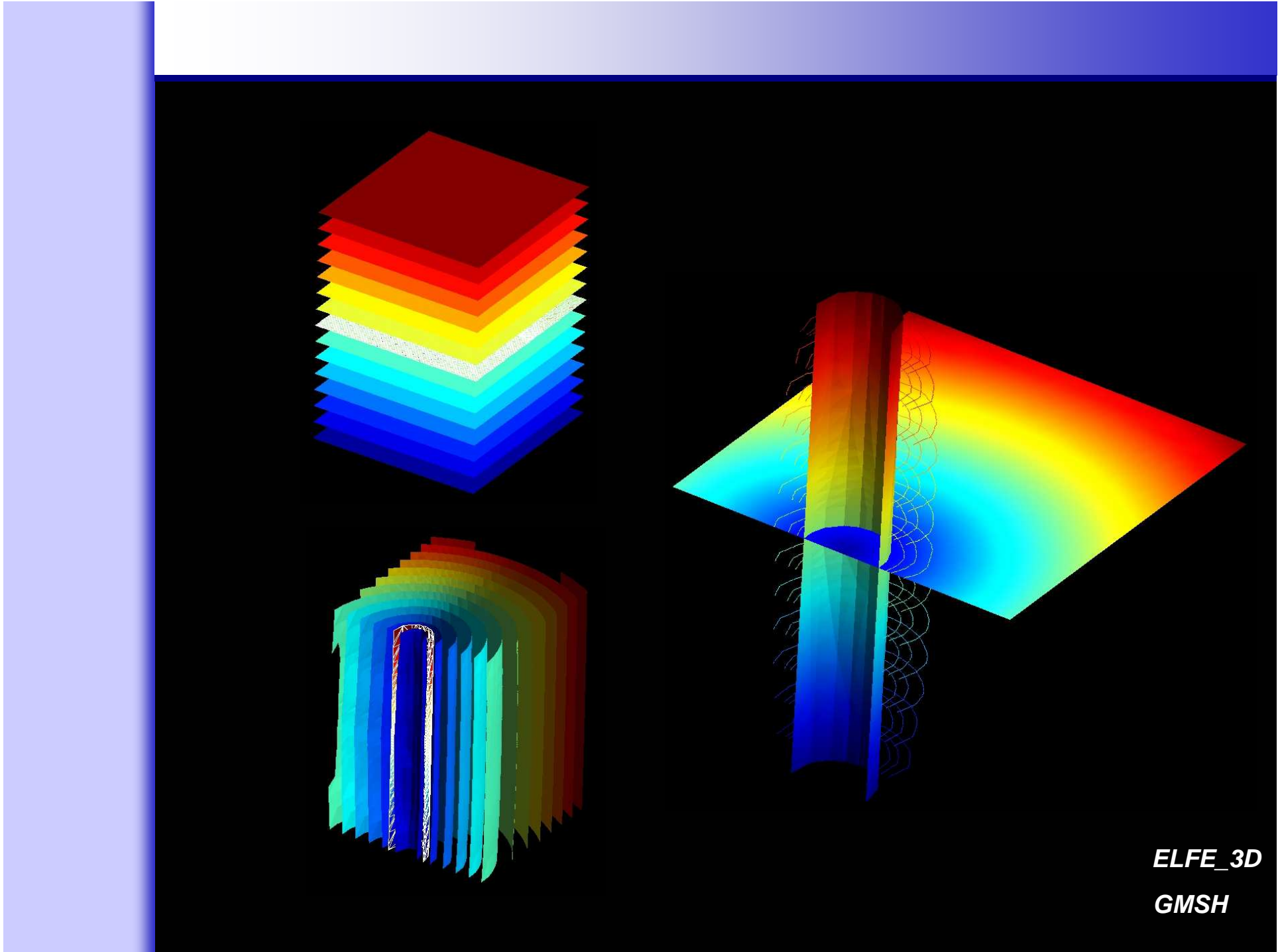
$$\begin{cases} \frac{\partial \phi}{\partial t} + H(\nabla \phi, \mathbf{x}, t) = 0 \\ \phi(\mathbf{x}, 0) = \phi_0(\mathbf{x}) \end{cases}$$

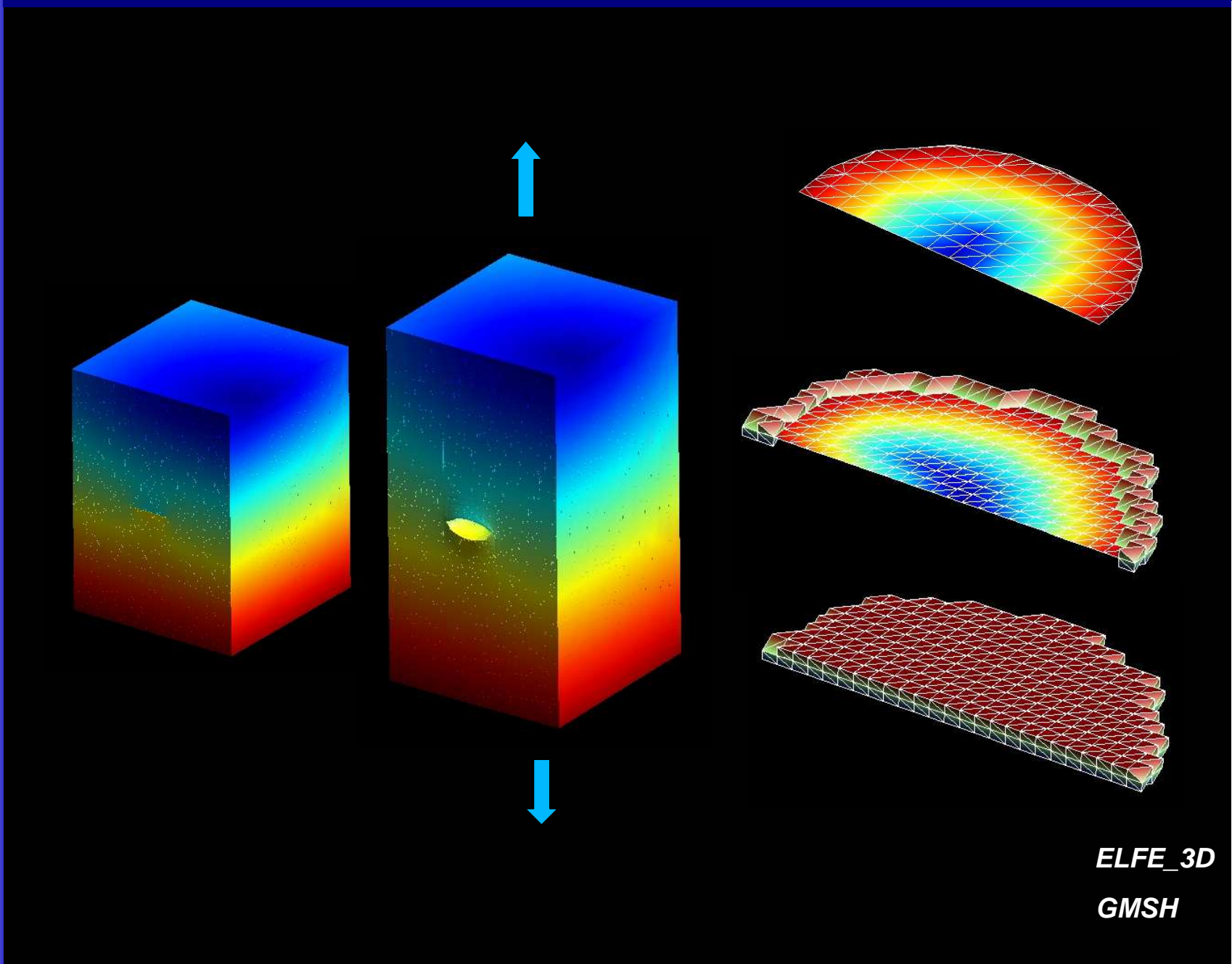
Space: [Barth and Sethian 1998]

Time: Runge Kutta



*Numerical schemes stable, accurate and convergent.
However, finite difference approaches are more accurate
for an equivalent size element mesh*





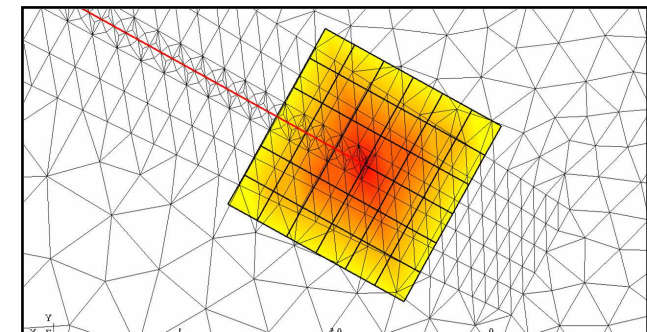
ELFE_3D
GMSH

Stress intensity factors calculation

2D interaction integral

$$I^{\Re,aux} = \int_C \left(W_l^{\Re,aux} \delta_{1j} - \sigma_{ij}^{\Re} \frac{\partial u_i^{aux}}{\partial x_1} - \sigma_{ij}^{aux} \frac{\partial u_i^{\Re}}{\partial x_1} \right) n_j \, ds + \sigma_{12}^{\Re}(A) [u_1^{aux}(A)]$$

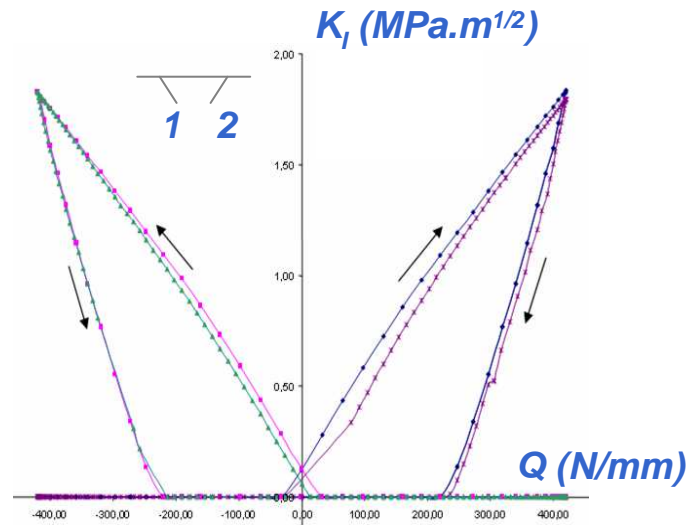
$$I^{\Re,aux} = \frac{2(1-v^2)}{E} \left(K_I^{\Re} K_I^{aux} + K_{II}^{\Re} K_{II}^{aux} \right)$$



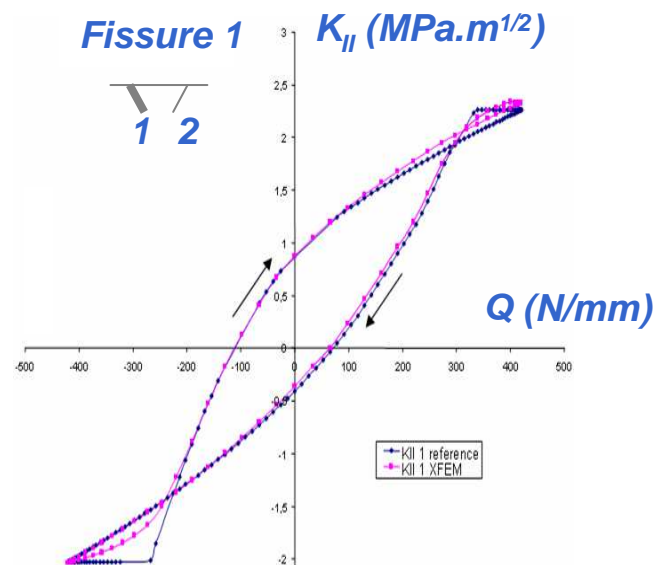
Integration domain close to the crack tip

Validation of the SIFs calculation:

Comparison with a semi-analytical model:[Dubourg et al, ASME J. Trib. 1992]



[M.C. Baietto, E. Pierres, A. Gravouil., IJSS 2010]



Critères prédisant la direction de propagation

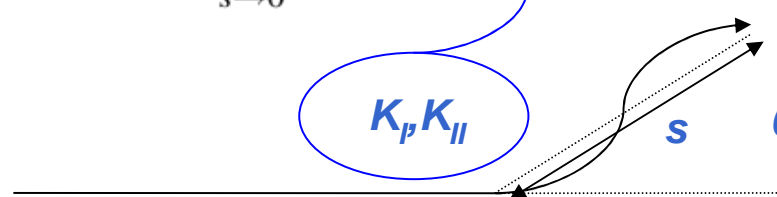
Calcul des contraintes des contraintes à l'extrémité infinitésimale d'une fissure (Amestoy et Leblond 1979) :

$$\begin{pmatrix} k_1^0(s, \theta) \\ k_2^0(s, \theta) \end{pmatrix} = \begin{bmatrix} K_{11}(\theta) & K_{12}(\theta) \\ K_{21}(\theta) & K_{22}(\theta) \end{bmatrix} \begin{pmatrix} K_I \\ K_{II} \end{pmatrix}$$

$$k_1^*(\theta) = \lim_{s \rightarrow 0} k_1^0(s, \theta)$$
$$k_2^*(\theta) = \lim_{s \rightarrow 0} k_2^0(s, \theta)$$

$$\left. \begin{array}{l} k_1^*(\theta) \\ k_2^*(\theta) \end{array} \right\}$$

→ Max $k_1^*(\theta)$
→ $k_2^*(\theta)$

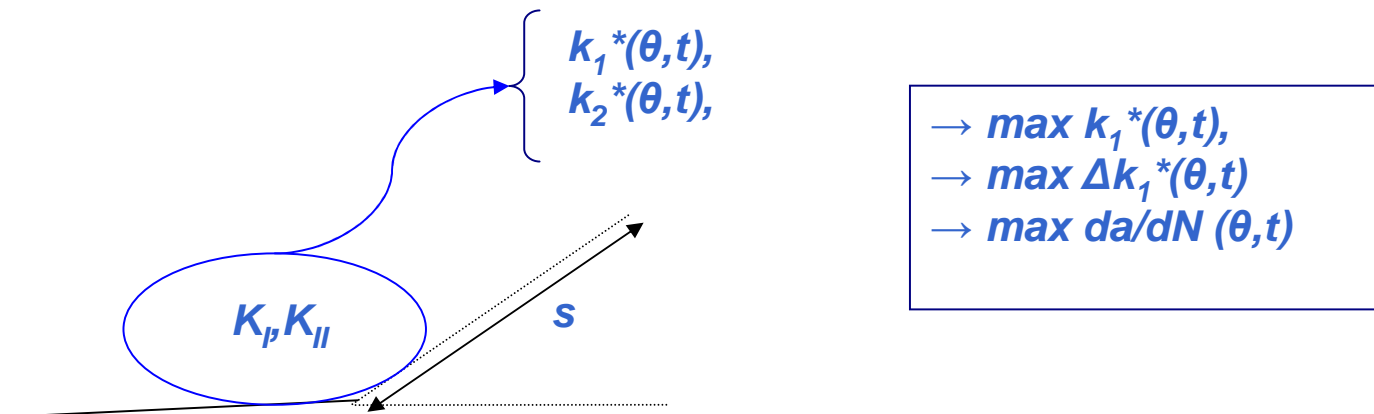


Critère basé sur les maximums des quantités calculés

Applicable à des chargements multi-axiaux proportionnels

Critères prédisant la direction de propagation

Extension des développements d'Amestoy par Pineau et Hourlier (1982)



3 critères basés sur les maximums en espace et en temps sur un cycle entier

Critère applicable à des chargements multi-axiaux non proportionnels